TKK Radio Science and Engineering Publications
Espoo, May 2010 REPORT R15

SYNCHROTRON EMISSION FROM BLAZAR JETS – ENERGY DISTRIBUTIONS AND RADIO VARIABILITY

Thesis for the degree of Doctor of Science in Technology

Elina Nieppola

Dissertation for the degree of Doctor of Science in Technology to be presented with due permission of the Faculty of Electronics, Communications and Automation, for public examination and debate in Auditorium S4 at Aalto University School of Science and Technology (Espoo, Finland) on the 28th of May, 2010, at 12 noon.

Aalto University
School of Science and Technology
Faculty of Electronics, Communications, and Automation
Department of Radio Science and Engineering

Cover: An artist's view of a blazar and its jets. (Steffen, W. 2010. www.cosmovision.com.mx, 20.4.2010)

Distribution:
Aalto University School of Science and Technology
Department of Radio Science and Engineering
P.O. Box 13000
FI-00076 AALTO
Tel. +358 9 470 22261
Fax +358 9 470 22267
E-mail ari.sihvola@tkk.fi

ISBN 978-952-60-3153-8 (paper)
ISBN 978-952-60-3154-5 (electronic)
ISSN 1797-4364 (paper)
ISSN 1797-8467 (electronic)

Aalto-yliopisto,
Aalto-Print
Helsinki 2010

Aalto University

ABSTRACT OF DOCTORAL DISSERTATION	AALTO UNIVERSITY SCHOOL OF SCIENCE AND TECHNOLOGY P.O. BOX 11000, FI-00076 AALTO http://www.aalto.fi

Author Elina Nieppola

Name of the dissertation

Synchrotron emission from blazar jets – energy distributions and radio variability

Manuscript submitted 22.12.2009	Manuscript revised 21.4.2010

Date of the defence 28.5.2010

☐ Monograph ☒ Article dissertation (summary + original articles)

Faculty	Faculty of Electronics, Communications and Automation
Department	Department of Radio Science and Engineering
Field of research	Radio astronomy
Opponent(s)	P. D. Silke Britzen
Supervisor	Prof. Martti Hallikainen
Instructor	Prof. Merja Tornikoski

Abstract

This thesis studies the synchrotron radiation of blazars from two perspectives: the spectral energy distributions, and radio emission and its variability. The first gives insight to the stable continuum emission originating in blazar jets, while the latter tells about the ephemeral events occuring in the jet flow, causing an outburst of radiation. The main goal is to establish the typical range of synchrotron emission properties for the fragmented blazar population, and use those data to test for any correlation between the wavelength of maximum synchrotron energy and source luminosity.

We determined the synchrotron peak frequencies and luminosities for two samples of blazars using a parabolic fit to archival data. The first was a very large sample of BL Lacertae objects (BLOs) and the second a complete sample of northern 1 Jy active galactic nuclei (AGN), for which we studied especially the Doppler-corrected properties. The range of synchrotron peak frequencies varied from the infrared to X-ray domain, and their distribution was smooth. Neither sample exhibited anti-correlation between the peak frequency and peak luminosity, contrary to the so-called blazar sequence scenario. In fact, when the Doppler-correction is properly applied, the two quantities have a positive correlation. This result was unexpected, but helps solve some inconsistencies in previous blazar research. It will also shed light on the relationship between the spectral energy distributions (SED) and the physics of the nucleus, as well as allows us to link the SED shape to other fundamental jet parameters, such as the jet speed and viewing angle.

To find the limits of the typical BLO radio behaviour, we observed a sample of almost 400 BL Lacertae objects in Metsähovi Radio Observatory for almost 4 years. Typically, BLOs are faint at 37 GHz, as only a third of the sample was detected at $S/N > 4$. However, there are also very bright and variable objects, which were studied in two separate works. Their radio flux curves were examined at several frequencies and their flaring behaviour determined, both individually and with respect to other subgroups of AGN. When the variable radio emission of blazars is considered, the range of typical behaviour is very large. The bright sources have intense flares of up to 50 Jy. The average flare duration is 2.5 years at 22 and 37 GHz.

Keywords	Active galactic nuclei, blazars, radio astronomy, spectral energy distributions	
ISBN (printed)	978-952-60-3153-8	ISSN (printed) 1797-4364
ISBN (pdf)	978-952-60-3154-5	ISSN (pdf) 1797-8467
Language	English	Number of pages 62 p. + app. 97 p.
Publisher	Aalto University Department of Radio Science and Engineering	
Print distribution	Aalto University Department of Radio Science and Engineering	

☒ The dissertation can be read at http://lib.tkk.fi/Diss/2010/isbn9789526031545

Aalto-yliopisto

VÄITÖSKIRJAN TIIVISTELMÄ	AALTO-YLIOPISTO TEKNILLINEN KORKEAKOULU PL 11000, 00076 AALTO http://www.aalto.fi

Tekijä Elina Nieppola

Väitöskirjan nimi

Blasaarisuihkujen synkrotroniemissio – energiajakaumat ja radiomuuttuvuus

Käsikirjoituksen päivämäärä 22.12.2009	Korjatun käsikirjoituksen päivämäärä 21.4.2010
Väitöstilaisuuden ajankohta 28.5.2010	
☐ Monografia	☒ Yhdistelmäväitöskirja (yhteenveto + erillisartikkelit)

Tiedekunta	Elektroniikan, tietoliikenteen ja automaation tiedekunta
Laitos	Radiotieteen ja -tekniikan laitos
Tutkimusala	Radioastronomia
Vastaväittäjä(t)	Dos. Silke Britzen
Työn valvoja	Prof. Martti Hallikainen
Työn ohjaaja	Prof. Merja Tornikoski

Tiivistelmä

Väitöskirjassa tutkitaan blasaarien synkrotronisäteilyä kahdesta näkökulmasta: spektrin energiajakaumien sekä radiosäteilyn ja sen muuttuvuuden kautta. Energiajakaumat kertovat suihkun stabiilista kontinuumisäteilystä, kun taas muuttuva radiosäteily kuvastaa suihkun lyhytaikaisia häiriöitä, jotka aiheuttavat purkauksia. Päätavoite on määrittää synkrotroniemission rajat blasaaripopulaatiolle ja saatujen tulosten avulla selvittää, onko synkrotronisäteilyn maksimienergian taajuus riippuvainen kohteen luminositeetista.

Määritimme synkrotronisäteilyn huipputaajuudet ja -luminositeetit kahdelle otokselle sovittaen paraabelifunktion arkistoista ja kirjallisuudesta kerättyihin havaintopisteisiin. Ensimmäinen otos käsitti lähes 400 BL Lacertae kohdetta (BL Lac), ja toiseen otokseen kuuluivat kaikki 1 Jy:n vuontiheysrajan ylittävät pohjoiset aktiiviset galaksinytimet. Jälkimmäisille tutkimme erityisesti Doppler-korjattuja ominaisuuksia. Synkrotronikomponentin huipputaajuus vaihteli infrapuna-alueelta röntgenalueelle, ja taajuuksien jakauma oli tasainen. Kummassakaan otoksessa ei todettu negatiivista korrelaatiota huipputaajuuden ja -luminositeetin välillä, vastoin nk. blasaarisekvenssin ennustusta. Itse asiassa, kun Doppler-korjaus otetaan huomioon, suureiden välillä on positiivinen korrelaatio. Tämä tulos oli odottamaton, mutta auttaa selvittämään epäjohdonmukaisuuksia aiemmissa tutkimuksissa. Se myös valottaa spektrin energiajakauman ja ytimen fyysisten ominaisuuksien välistä suhdetta, ja mahdollistaa energiajakauman ominaisuuksien vertaamisen muihin suihkun perusparametrihin, kuten nopeuteen ja katselukulmaan.

Löytääksemme BL Lacien tyypillisen radiokäyttäytymisen rajat havaitsimme melkein 400 kohteen otosta Metsähovin radiotutkimusasemalla lähes neljän vuoden ajan. Useimmiten BL Lacit ovat himmeitä 37 GHz:in taajuudella, koska vain kolmannes otoksen kohteista detektoitiin ($S/N > 4$). Osa on kuitenkin radiokirkkaita ja muuttuvia, ja niitä kohteita tutkittiin kahdessa erillisessä tutkimuksessa. Määritimme vuontiheyskäyrät monella radiotaajuudella ja tutkimme purkauskäyttäytymistä sekä erikseen yksittäisille kohteille että BL Laceille verrattuna muihin aktiivisten galaksinytimien alaluokkiin. Muuttuvan radiosäteilyn vaihteluväli on erittäin suuri. Kirkkaimmat kohteet saattavat purkauksen aikana saavuttaa jopa 50 Jy:n vuontiheyden. Keskimäärin purkaukset kestävät 2.5 vuotta 22 ja 37 GHz:in taajuuksilla.

Asiasanat Aktiiviset galaksinytimet, blasaarit, radioastronomia, spektrin energiajakaumat

ISBN (painettu) 978-952-60-3153-8	ISSN (painettu) 1797-4364
ISBN (pdf) 978-952-60-3154-5	ISSN (pdf) 1797-8467
Kieli Englanti	Sivumäärä 62 s. + liit. 97 s.

Julkaisija Aalto-yliopiston radiotieteen ja -tekniikan laitos

Painetun väitöskirjan jakelu Aalto-yliopiston radiotieteen ja -tekniikan laitos

☒ Luettavissa verkossa osoitteessa http://lib.tkk.fi/Diss/2010/isbn9789526031545

Preface

These past five years have gone by quickly, and it feels like I started my thesis work only yesterday. I have enjoyed the journey, and it is time to thank those who have made it possible.

The thesis research was carried out at the Metsähovi Radio Observatory of Aalto University. I gratefully acknowledge the funding from the Finnish Graduate School in Astronomy and Space Physics and the Academy of Finland.

The biggest thanks goes to my instructor, Prof. Merja Tornikoski. I am grateful for the opportunity to be a part of the Metsähovi team, and for all the support during these years. The same goes for Prof. Esko Valtaoja, who has acted as a second instructor, and always has an answer to any question. I would also like to thank the whole Metsähovi-Tuorla AGN group, especially Talvikki Hovatta, Ilona Torniainen and Anne Lähteenmäki, for the support and also the conference trips! I think Metsähovi has an exceptionally relaxed atmosphere and it is a pleasure to work there. I hope it will stay that way for many years to come. Thanks to the whole Metsähovi staff!

Family and friends deserve my gratitude for keeping my mind off science when not at work. Erikoiskiitos Jussille ja Veikalle!

Espoo, April 2010

Elina Nieppola

Contents

List of Publications

This thesis consists of an overview and of the following publications which are referred to in the text by their Roman numerals.

I **Nieppola, E.**, Tornikoski, M. and Valtaoja, E.:
"Spectral energy distributions of a large sample of BL Lacertae objects",
Astronomy & Astrophysics, Vol. 445, pp. 441-450, 2006 .

II **Nieppola, E.**, Tornikoski, M., Lähteenmäki, A., Valtaoja, E., Hakala, T., Hovatta, T., Kotiranta, M., Nummila, S., Ojala, T., Parviainen, M., Ranta, M., Saloranta, P.-M., Torniainen, I. and Tröller, M.:
"37 GHz observations of a large sample of BL Lacertae objects",
The Astronomical Journal, Vol. 133, pp. 1947-1953, 2007.

III Hovatta, T., **Nieppola, E.**, Tornikoski, M., Valtaoja, E., Aller, M. F. and Aller, H. D.:
"Long-term radio variability of AGN: flare characteristics",
Astronomy & Astrophysics, Vol. 485, pp. 51-61, 2008.

IV **Nieppola, E.**, Valtaoja, E., Tornikoski, M., Hovatta, T. and Kotiranta, M.:
"Blazar sequence - an artefact of Doppler boosting",
Astronomy & Astrophysics, Vol. 488, pp. 867-872, 2008.

V **Nieppola, E.**, Hovatta, T., Tornikoski, M., Valtaoja, E., Aller, M. F., Aller, H. D.:
"Long-term variability of radio-bright BL Lacertae objects",
The Astronomical Journal, 2009, Vol. 137, pp. 5022-5036, 2009.

Author's contribution

In Paper I, Paper II and Paper IV the author had the main responsibility for compiling the data, making the analyses, interpreting the results and writing the paper. In Paper III the author participated in the data analyses and the interpretation of the results. In Paper V the author was responsible for the most of the data analyses, interpretation and writing of the article. Compiling the data and the decomposition of the flux curves into flares was done by T. Hovatta.

List of Abbreviations

AGN	Active Galactic Nucleus or Active Galactic Nuclei
BLO	BL Lacertae Object
BLR	Broad Line Region
CMB	Cosmic Microwave Background
DCF	Discrete Correlation Function
DXRBS	Deep X-ray Radio Blazar Survey
EC	External Compton
EXOSAT	European X-ray Observatory Satellite
FR I	Fanaroff-Riley type I galaxy
FR II	Fanaroff-Riley type II galaxy
FSRQ	Flat Spectrum Radio Quasar
HBL	High-energy BL Lac Object
HFSRQ	High-energy Flat Spectrum Radio Quasar
HPQ	Highly Polarised Quasar
IBL	Intermediate BL Lac Object
IC	Inverse Compton
LBL	Low-energy BL Lac Object
LPQ	Low Polarisation Quasar
NLR	Narrow Line Region
RBL	Radio-selected BL Lac Object
RGB	ROSAT All-sky - Green Bank Survey
ROSAT	The Roentgen Satellite
SED	Spectral Energy Distribution
SF	Structure Function
SSC	Synchrotron Self-Compton
UMRAO	University of Michigan Radio Astronomy Observatory
UV	Ultraviolet
VLBI	Very Long Baseline Interferometry
XBL	X-ray-selected BL Lac Object

List of Symbols

B	Strength of the magnetic field
c	Speed of light
D	Doppler boosting factor
E	Energy
e	Electron charge
G	Gravitational constant
H_0	The Hubble Constant
L	Luminosity
M	Mass
$\dot{M}$	Accretion rate
m	Electron mass
P	Power
P_{pol}	Degree of polarization
R	Radius
R_s	Schwarzschild radius
S	Flux density
U_B	Energy density of the magnetic field
U_{ph}	Energy density of the photon field
V_{varI}	Variability index
V_{varII}	Variability index
z	Redshift

α	Spectral index
β	Speed of a component in the jet
$\beta_{\rm app}$	Apparent speed of a component in the jet
Γ	Bulk Lorentz factor of the jet
γ	Lorentz factor of a single particle in the jet
γ_{peak}	Peak electron energy
η	Radiative efficiency
θ	Viewing angle
λ	Wavelength
ν	Frequency
ν_g	Gyration frequency
ν_p	Synchrotron peak frequency
ϕ	Jet opening angle

1 Introduction

The dark night sky is filled with small specks of light, all similar to the human eye. However, they are not the same: the objects we see are stars of various kinds, planets, even galaxies for the sharp-eyed. The photons that make up the light we see tell a story of the physical conditions of their place of origin and of the medium they have travelled through. When we use a telescope to amplify the radiation, suddenly the sky is teeming with even more exotic objects. Now we see objects further away, whose light has been travelling for millions of years in space. There is a multitude of distant galaxies, spiral, elliptical and irregular, including one that looks like a cartwheel. Among this zoo, there is a peculiar group of galaxies that harbour a massive black hole in their centre. The giant slowly eats away at the gas of its host galaxy, and in doing so shines more brightly than all the stars of its host combined. Some of these extraordinary objects have massive outflows emanating symmetrically from their centre, shooting out material far into intergalactic space. As exceptional as this sounds, there are thousands of these gigantic, active galaxies. They are all very distant, which equals old. When looking at them, we see into the past of our universe. The most extreme of these objects are called blazars, which is descriptive of their variable behaviour.

Besides helping us to see deeper and clearer, the telescope can also help us see at different wavelengths. The visible light that our eyes are designed to receive and process is only a thin slice of the electromagnetic spectrum. Visible light is made of photons of a certain energy; when that energy is lower, we have radio or infrared radiation, and when that energy is higher, we have ultraviolet, X-ray or gamma radiation. All these wavelengths can be observed using an appropriate instrument. Celestial objects often radiate most of their energy in frequencies other than optical. If our eyes could see the night sky in radio wavelengths, blazars would be among the brightest objects in spite of their distance. They would shine like luminous beacons, and the sky would never look exactly the same on two nights due to the variations in their brightness.

Blazars and their multifrequency behaviour are the subject of this thesis. They may be invisible to the odd sky-gazer on Earth due to their distance, but at radio, X-ray, and gamma regimes blazars are major players. Blazar science is relatively new. The archetype of the class, BL Lacertae, was discovered only 40 years ago. In 1996, the number of known blazars was already hundreds, and in a recent catalogue (Massaro et al. 2009) the number was 2728. Still, this is only 2 % of all active galaxies. Blazars offer a unique environment to study strong, large-scale magnetic fields in the vicinity of a black hole and test magnetohydrodynamical models. They are also major contributors to the background radiation in radio, X-ray, and gamma frequencies.

This thesis approaches blazars from two different view points: investigating their total energy output from the radio to X-ray frequencies, and their radio emission and its variability on a time scale of years or decades. This way we gain knowledge on both the stable emission of a blazar as well as on more transient events causing the variability. The main motivation behind this research is to establish the common properties of the inhomogeneous blazar population of today, or, where commonalities cannot be found, set limits on

the typical behaviour. With the exponential increase in the astronomical data in the last decades, new sources are discovered by the hundreds using different techniques. Usually, the research concentrates on limited samples from the new surveys. While these studies are necessary and valid, the quickly expanding population as a whole slowly diverges and becomes nearly unmanageable. This thesis is an attempt to reduce that chaos.

The overview part of this thesis is organized as follows: Sect. 2 introduces the blazars and their unique properties, Sect. 3 describes the emission processes in blazars and the shape of the energy distribution that results, Sect. 4 outlines the possible relations of the energy distribution to physical properties of the object and Sect. 5 discusses the typical radio variability in blazars and processes that produce it. Conclusions are drawn in Sect. 6 and the thesis publications are summarized in Sect. 7.

2 The blazar phenomenon

2.1 The AGN framework

Active galactic nuclei (AGN) are the most exotic and powerful of celestial objects. They are the core regions of normal galaxies that outshine the combined starlight from the whole galaxy. The central engine producing this vast amount of energy is a supermassive ($M \gtrsim 10^9 M_{sun}$) black hole (SMBH) which is surrounded by an accretion disk of infalling matter. The presence of an SMBH has been deduced from many pieces of evidence. Ford et al. (1994) measured the gas velocities near the core of the radio galaxy M87. The gas dynamics could only be explained by a central black hole of the mass $2.4 \pm 0.7 \times 10^9 M_{sun}$. Similarly, rotating gas at high velocities was discovered by Miyoshi et al. (1995). They detected highly blue- and redshifted H_2O megamaser emission from the galaxy NGC 4258. They derived a mass of $3.6 \times 10^7 M_{sun}$ concentrated in a 0.13 pc radius. The nearest SMBH resides in the centre of our own galaxy. It has a relatively low mass of $4.31 \times 10^6 M_{sun}$ (Gillessen et al. 2009). The presence of an SMBH is also revealed by the rapid flux density variability exhibited by some AGN. The relatively short time scale of the variability severely limits the size of the emitting region. Combined with the knowledge that the central area is very massive, an SMBH is the only viable explanation.

The accretion onto the supermassive black hole is a powerful process producing a wealth of thermal radiation, mainly optical and UV. The luminosity, L, produced by the accretion is

$$L = \eta \dot{M} c^2, \tag{2.1}$$

where η is the radiative efficiency, $\dot{M}$ is the accretion rate, and c is the speed of light. As the matter falls in, the radiation from the accretion escapes out. This sets an upper limit for the luminosity: the radiation pressure cannot exceed the gravity. This upper limit is called the Eddington luminosity

$$L_E = 4\pi G M m_p c / \sigma_T, \tag{2.2}$$

where G is the gravitational constant, M is the mass of the black hole, m_p is the mass of a proton and σ_T is the Thompson cross-section.

AGN are distant objects, their redshift distribution extending up to ~ 6. They have a positive cosmological evolution (Hopkins et al. 2007), which means that they tend to be more numerous in the early universe. The space density shows a peak at $z = 2 - 3$ and at higher z AGN are rarer again. Through a process not very well understood, in roughly 10 % of cases the nucleus also launches symmetrical jets of matter and radiation (de Vries et al. 2006), emanating from the core and extending on the scale of kiloparsecs into the intergalactic space. Fig. 2.1 presents a schematic diagram of the structure of an AGN. The accretion disk and the black hole are surrounded by an obscuring molecular torus. Although in the figure the torus is dougnut-shaped, its precise form is not clear. Other suggestions include a flared disk (Fritz et al. 2006), tapered disks (the disk height increases up to a certain radius, but tapers off to a constant height in the outer parts) (Efstathiou & Rowan-Robinson 1995) and a clumpy torus (Nenkova et al. 2008). Inside the

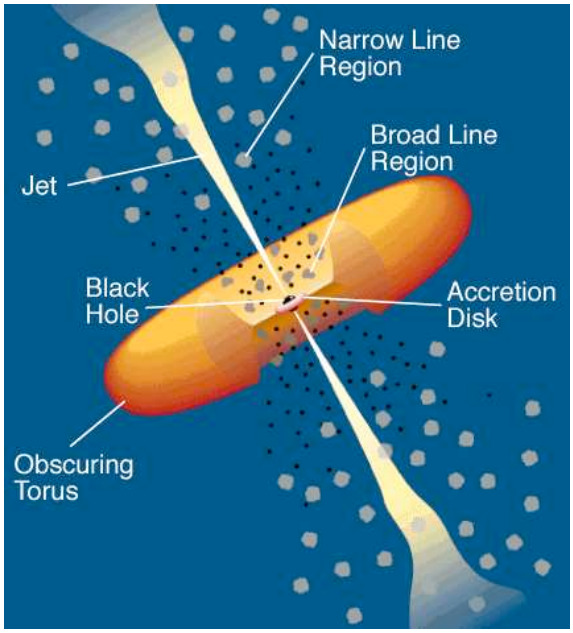

Figure 2.1: A basic diagram of AGN anatomy. (Urry & Padovani 1995)

torus, near the central engine, is the broad line region (BLR). The BLR is an absorption region that produces broad lines in the source continuum spectrum, i.e., the absorbing gas is moving at high velocities. The BLR can be used to determine the mass of the central black hole. In a process called reverberation mapping the size of the BLR and the velocity of the BLR clouds determine the central mass when Keplerian motion is assumed. Further down in the direction of the jet there is the narrow line region (NLR), producing narrower absorption lines. Narrow line emission can extend far from the core (roughly 10 pc), and in that case it is called extended narrow line region (ENLR). Some AGN feature also radiation from very highly ionized elements. It originates from the coronal line region (CLR), which may be located between the BLR and NLR, but may also consist of several components.

The asymmetrical geometry of an AGN means that the observer's perception of it depends on the direction from which she is observing, i.e., the line of sight. If the AGN is viewed perpendicular to the jet axis, the central region and the BLR are hidden from view by the dusty molecular torus. The jets, in turn, are spectacularly visible. If the observer's line of sight coincides with the jet axis, the source appears core-dominated. The radiation from the approaching jet is relativistically boosted (discussed in Sect. 2.2) and completely dominates the AGN emission. According to the so-called unified schemes (Urry & Padovani 1995) the various subclasses of AGN can be accounted for by changing the line of sight. BL Lacertae objects are one of these subclasses, their name originating from the archetype of the class. BL Lacertae was thought to be a variable star in the constellation of Lacerta until the late 1960's, when it was associated with the radio source VRO 42.22.01 (Schmitt 1968) and realised to be of extragalactic origin. These objects

are typically viewed from small angles with respect to the jet. The parent population is thought to be mostly Fanaroff-Riley type I radio galaxies, although this scenario has been doubted recently. A small viewing angle with respect to the jet causes BL Lacertae objects to have many extreme properties, discussed in detail in Sect. 2.3.1.

2.2 Relativistic jets

Jets originating from spinning accretion disk systems are a common phenomenon in astrophysics. Their scale varies from the jets of micro-quasars and young stellar objects (1 pc) to those of AGN (1 Mpc). AGN and their jets are the largest coherent objects in the universe.

The processes involved in the launching of the jets from the core of the AGN are poorly understood. There are, however, some features that are widely accepted (Marscher (2009) offers a review). Most of the acceleration of blazar jets occurs inside a 10 pc radius. Sikora et al. (2005) concluded that Lorentz factors of $\gamma \sim 10$ should be reached on scales $\lesssim 10^{17}$cm. This large-scale acceleration indicates the presence of strong magnetic fields and invokes the need for magnetohydrodynamic models, as pure hydrodynamic acceleration would saturate on much shorter distances (Vlahakis & Königl 2004, Königl 2007). It is thought that the differential rotation of the ergosphere of the spinning black hole winds the magnetic field lines into a helix. The plasma flows along these field lines, shooting out from the core. The power needed to accelerate the plasma could be extracted from the accretion process and/or the black hole spin (Blandford & Znajek 1977, Blandford & Payne 1982). The toroidal component of the magnetic field provides a pinching force directed towards the jet axis, while a pressure gradient parallel to the axis accelerates the plasma further. Thus, the jet is initially dominated by the Poynting (i.e., magnetic) flux. It is likely that at some distance from the core the jet becomes matter-dominated. The energy content of electrons (and positrons, if any) is too low, so the jet dynamics are dominated by protons, although the number of leptons greatly exceeds the number of protons (Sikora et al. 2005). From this point forward, the jet plasma is no longer accelerated by the magnetic field, but is in a ballistic motion. It has been suggested that there is a radial velocity gradient in the jet, i.e., the inner jet flows faster than the surface layer (so-called spine-sheath structure, Perlman et al. 1999, 2001, Giroletti et al. 2004). This would be useful in explaining the slow motion of the TeV-emitting jets. The energetic gamma-rays would originate in the fast spine, and the radio emission in the slower surface layer (e.g., Ghisellini et al. 2005) .

Fig. 2.2 shows the inner jet anatomy and the emission sites. After the acceleration and collimation zone, the helical magnetic field takes on a more chaotic form. At roughly 1 pc from the central engine there is a radio core, where the jet becomes visible in the radio frequencies. Recent research suggests that the radio core is a standing shock (D'Arcangelo et al. 2007), although it could also be the point where radio emission simply stops being self-absorbed and becomes optically thin. In addition, there are moving shocks (superluminal knots) travelling in the jet, which are understood to be the main generators of the flux density variability in AGN (these are discussed in more detail in Sect. 5.1). The scale of the acceleration region with respect to the whole jet is worth noting: it is of the order

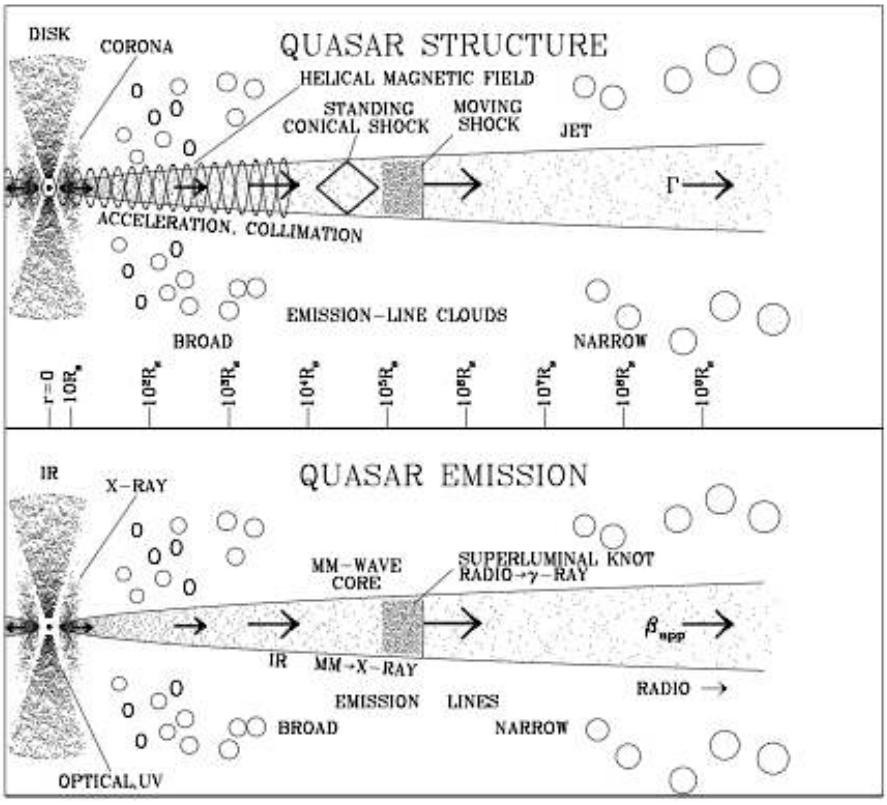

Figure 2.2: A schematic figure of a quasar jet and relevant emission. (Marscher 2009)

of $10^3 - 10^4 R_s$ [1] (Sikora et al. 2005, Krolik 2008). Thus, it is completely shrouded by the molecular torus surrounding the central engine, and represents a small fraction of the whole jet length. Radio emission, which is the main focus of this dissertation, originates from the mm-wave core all the way to the downstream end of the jet, kiloparsecs away. Along the jet's length, the particle density decreases as the collimating helical magnetic field diminishes, and the frequency of the emitted radiation decreases as well. Often the jets end in extended areas of low-frequency radio emission.

AGN with jets are traditionally categorized by the strength of their radio emission and morphology in two classes (Fanaroff & Riley 1974). Fanaroff-Riley type I galaxies (FRI) have continuous jets that grow fainter with increasing distance from the core and may have significant bends. In type II galaxies (FRII) the jets themselves are faint, but end in striking radio lobes, or "hot spots". Thus, FRI's are brightest in their centre, and FRII's are brighter toward the edges. Figure 2.3 depicts their different morphologies. FRI's are also clearly lower in luminosity, the dividing line at 178 MHz being $L_{\mathrm{FRI}} < 2 \times 10^{25} h_{100}^{-2} \mathrm{W\,Hz^{-1}str^{-1}} < L_{\mathrm{FRII}}$, where $h_{100} = H_0/100$ is Hubble's constant. It appears that FRII's are more efficient in transporting energy to the lobes, whereas FRI's radiate

[1] R_s is the Schwarzschild radius, defined by $R_s = \frac{GM}{c^2}$.

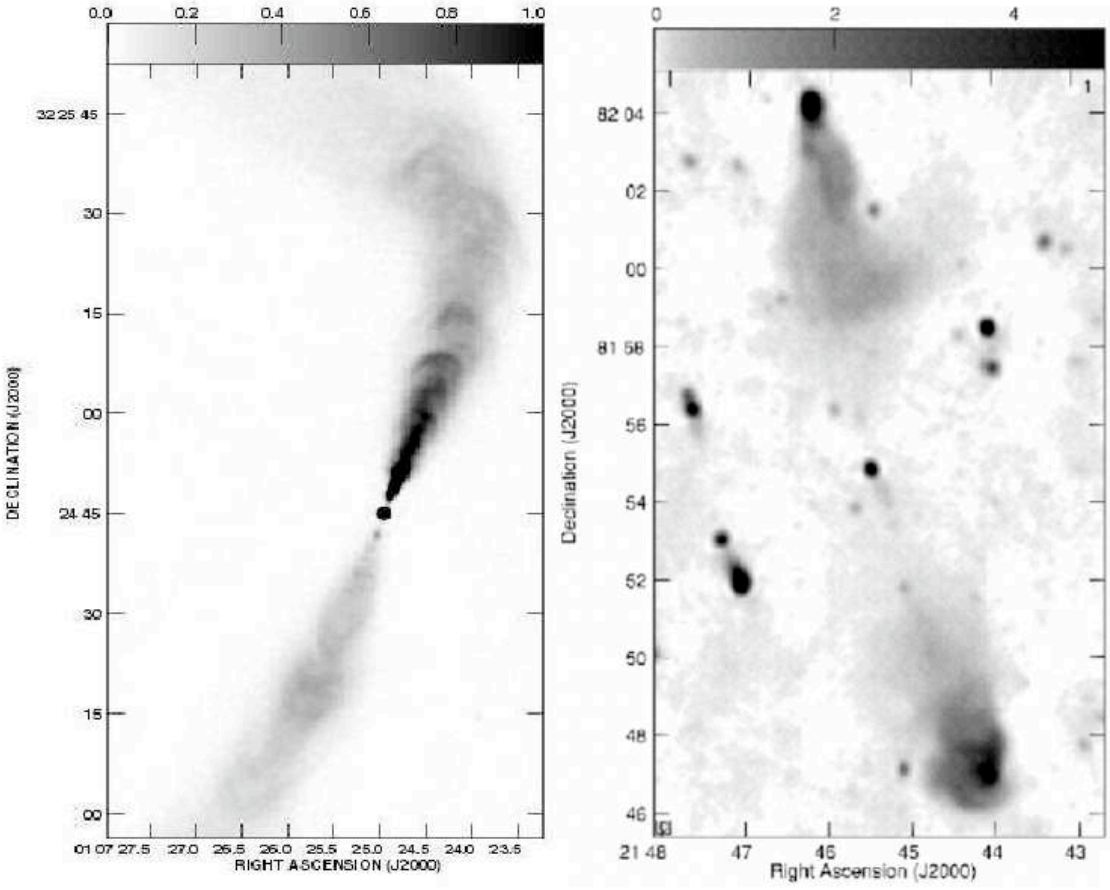

Figure 2.3: Examples of FR type I at 8.4 GHz (left) and type 2 at 1.4 GHz (right) radio galaxies. The sources are 3C 31 and NVSS 2146+82, respectively. The lobe-dominated morphology of FRII galaxies compared to FRI's shows clearly. (Left: Laing et al. (2008), right: Palma et al. (2000))

their energy along the jet's length. A possible reason for this are the different properties of the medium through which the jet travels.

The extreme nature of AGN on an astronomical scale evokes the need to consider relativistic effects when observing them. The one affecting continuum observations the most is relativistic beaming, or Doppler boosting. The boosting concept was first discussed by Blandford & Königl (1979). Fig. 2.4 shows the main parameters of the AGN jet system: the jet opening angle, ϕ, and the viewing angle, θ, i.e., the angle between the jet and the observer's line of sight. The jet plasma is moving at a velocity β, which is given in units of c. Beaming effects become important when the viewing angle θ is small and the speed of the jet matter approaches the speed of light. In that case, due to geometrical effects, the matter in the jet appears to the observer to move at a superluminal speed. The idea of AGN jets exhibiting superluminal speeds was first put forward by Rees (1966). The

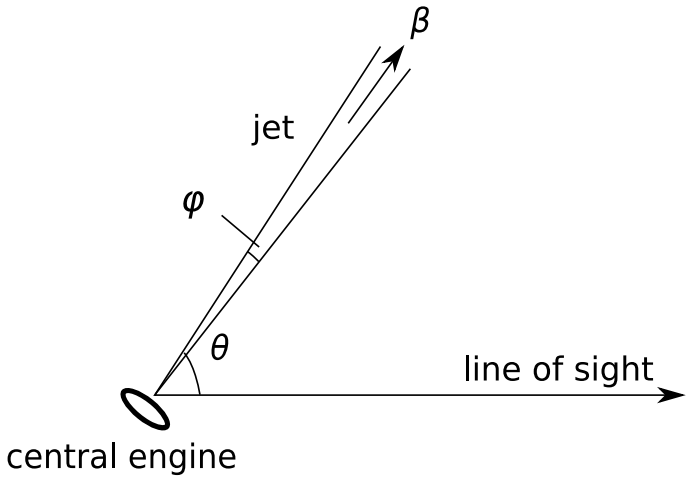

Figure 2.4: Main parameters of an AGN jet. A similar jet emanates from the other side of the central area, but is not included in the figure.

apparent speed of the jet, β_{app}, in units of the speed of light, can be calculated with the equation

$$\beta_{\mathrm{app}} = \frac{\beta \sin\theta}{(1 - \beta\cos\theta)}, \tag{2.3}$$

where β is the speed of the jet in the source's frame. For apparent superluminal motion to occur, β must be for example $0.75\,c$ or larger for $\theta = 40\,^{\circ}$.

The Doppler boosting factor D quantifies the significance of the boosting effect for the source, and can be presented as

$$D = [\gamma(1 - \beta\cos\theta)]^{-1}, \tag{2.4}$$

where $\gamma = (1 - \beta^2)^{-1/2}$ is the Lorentz factor corresponding to the jet velocity β. The main consequence from beaming is the boosting of the observed luminosity of the source. If the observer records a luminosity L_o, the rest frame luminosity of the moving plasma is

$$L_i = L_o \left(\frac{1+z}{D}\right)^{3+\alpha}, \tag{2.5}$$

where z is the redshift of the source and α is the appropriate spectral index. The spectral index is the slope of the continuum spectrum, when presented in the form $\log S$ vs. $\log \nu$. It can be expressed as

$$\alpha = \frac{\log(S_1/S_2)}{\log(\nu_1/\nu_2)}, \tag{2.6}$$

where S_1 and S_2 are the flux densities at frequencies ν_1 and ν_2, respectively. The spectral index is a basic quantity often referred to in AGN research. It is used to describe the slope of the spectrum both inside a certain frequency domain (e.g., radio spectral index), or be-

tween different wavelength regions of the electromagnetic spectrum (broadband spectral index). Eq. 2.5 assumes $S \propto \nu^{-\alpha}$.

Not all radiation components of an active galaxy are affected by beaming. The radiation originating in a stationary source, i.e., the host galaxy, is not boosted at all. The host galaxies of blazars, as those of quasars in general, are typically elliptical galaxies (Dunlop et al. 2003). In the presence of beaming jets, the host galaxy emission is often completely swamped and the radiation we observe is the non-thermal continuum radiation of the jets. Fig. 2.5 illustrates this fact: Landt et al. (2002) have simulated optical spectra of a BL Lacertae object (this AGN class introduced in detail in Sect. 2.3.1) when the jet/host galaxy emission ratio is changing from 0.2 to 100. The optical spectral slope of the simulated jet is $\alpha = 1$ ($S \propto \nu^{-\alpha}$). As the jet intensity relative to the galaxy increases, two things are evident in the figure: the galactic absorption features become weaker and the shape of the spectrum starts to resemble the $\alpha = 1$ continuum.

2.3 Members of the blazar family

As mentioned, the amount of Doppler boosting is heavily dependent on the viewing angle. For boosting to have a real impact on the source properties, the viewing angle has to be approximately $\theta < 20\,^{\circ}$. Thus, viewing angle being a free parameter, beamed objects form a minority among AGN. These luminous objects are called blazars. The definition of the class is not very stable, but typically they are thought to be beamed, variable AGN emitting radiation over the entire electromagnetic spectrum. Sometimes detected gamma-ray emission is added to the blazar criteria, but it is not prerequisite in this thesis. The term "blazar", first proposed by Edward A. Spiegel in 1978, is actually a combination of BL Lac object and quasar. These two, more accurately BL Lacertae objects and flat spectrum radio quasars, make up the blazar class. They are described in more detail in the following.

2.3.1 BL Lacertae objects

In the very first paper introducing BL Lacertae objects (BLOs) (Strittmatter et al. 1972), they are said to have

- rapid variations in intensity across the electromagnetic spectrum
- energy distributions that peak in the infrared wavelengths
- absence of emission lines in the optical spectra
- strong and rapidly varying radio and optical polarization.

Especially the lack of optical emission lines has traditionally been the hallmark of BLOs (Fig. 2.6). However, with the development of the observing equipment, the featureless spectra observed in the 1960's or 70's may be featureless no more. Due to the relative nature of this definition, the criterium was soon relaxed from strict absence of

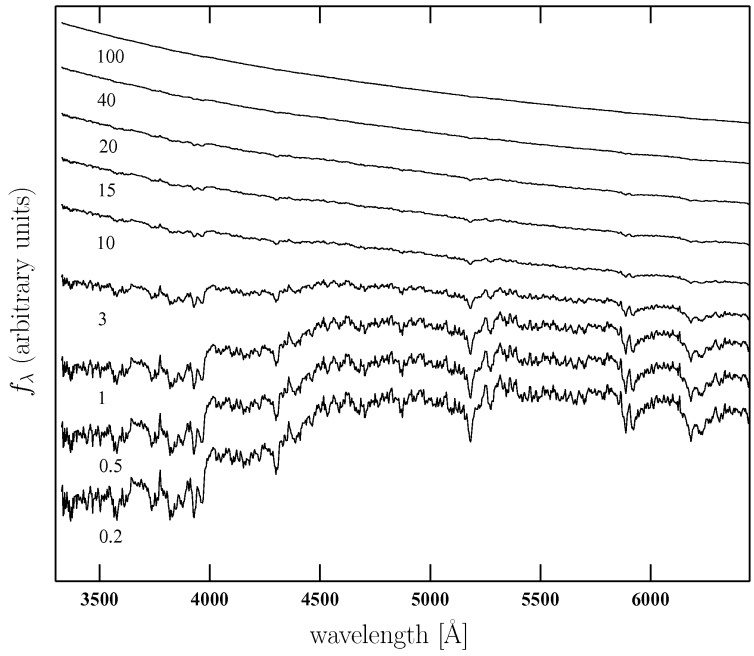

Figure 2.5: The behaviour of a simulated optical BL Lacertae spectrum with an increasing jet/galaxy emission ratio. (Landt et al. 2002)

emission lines. The traditionally adopted maximum equivalent width for BLO emission line is 5 Å. Alternatively, the emission features can be quantified with the CaII H&K -break. The break is a measure of the fractional change in the host galaxy continuum blueward and redward of 4000 Å and its value diminishes with increasing jet power. Its maximum value for BLOs has been taken to be 40 % (Marcha et al. 1996). Above this value the source emission becomes increasingly dominated by extended lobes and is no longer core-dominated (Landt et al. 2002). The CaII H&K -break can clearly be seen diminishing around λ = 4000 Å with the increasing jet dominance in the simulation of Fig. 2.5.

Although beaming has a masking effect that certainly contributes to the weak emission lines of BLOs, it cannot be the only factor. The reason must be at least partly intrinsic. The radiative properties of the accretion disk surrounding the black hole might be different from other AGN. Ghisellini et al. (2009) suggest that the accretion rate of BLOs is crucially lower that their strongly-lined counterparts. This leads to optically thin and radiatively inefficient accretion flow, and the surroundings of the accretion disk will be deprived of photons. Thus, the BLR is very weak. Another possibility is that the molecular torus, which reprocesses the thermal radiation from the accretion disk, is thinner or completely absent in BLOs. Kharb & Shastri (2004) find that the optical core luminosity of FRI galaxies is orientation dependent, which indicates that their tori are very weak at best. However, this result applies to BLOs as a class only if FRI's are their parent popu-

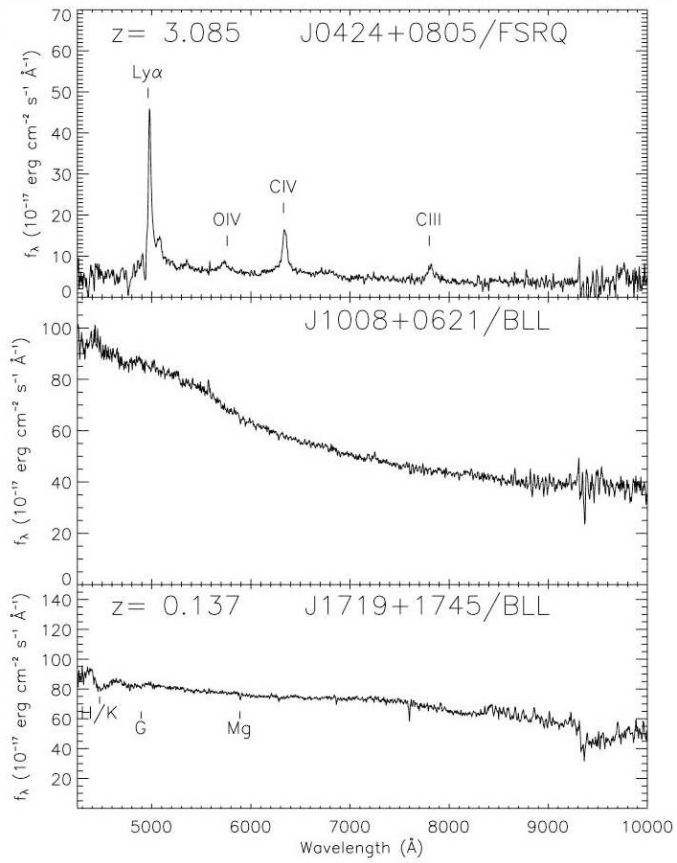

Figure 2.6: The optical spectra of two BL Lacertae objects (middle and bottom panels) compared to that of a flat-spectrum radio quasar (top panel). The absence of emission features in the BLO spectra is clearly depicted. (Sowards-Emmerd et al. 2005)

lation (see Sect. 2.3.2). It is likely that the absence of the emission lines in BLO spectra is the result of all these factors in different proportions.

In Strittmatter et al. (1972) the number of known BLOs was five. In the latest version of the Catalogue of quasars and active galactic nuclei by Veron-Cetty & Veron (2010), the number of definite or probable BLOs has risen to 1374 (still less than 1 % of all known AGN). BLOs are mainly discovered in radio or X-ray surveys. In the optical wavelengths it is very difficult to discern lineless AGN from the multitude of other optical sources. The radio domain is suitable for separating the optically star-like objects from normal stars, which do not emit in radio frequencies. Also, radio observations are technically relatively easy, unlike X-ray surveys which require spaceborne instruments. In X-ray region BLOs and other blazars are strong continuum emitters, which makes their detection easier.

The most notable classical radio surveys include the 1-Jy survey (Stickel et al. 1991, 1993), S4 (Pauliny-Toth et al. 1978, Stickel et al. 1994) and S5 surveys (Kühr et al. 1981, Kühr & Schmidt 1990, Stickel & Kühr 1996). In X-rays, most early identifications came

from the Einstein medium sensitivity survey (Gioia et al. 1990, Stocke et al. 1991, Maccacaro et al. 1994), EXOSAT (Giommi et al. 1991), Einstein slew survey (Perlman et al. 1996) and ROSAT all-sky survey (Bade et al. 1994). There are also some relatively recent optically selected BLO samples, like the 2BL sample (Londish et al. 2002, 2007) and the optically selected BLO candidates from the Sloan Digital Sky Survey (SDSS) (Collinge et al. 2005, Plotkin et al. 2009). Discovering new BLOs in the optical wavelengths is made difficult by their faint emission lines, which hinders the accurate estimation of their distance. However, their redshifts can also be estimated using the standard candle method used by Sbarufatti et al. (2005). The absolute magnitudes of BLO host galaxies are distributed narrowly enough to be considered as standard candles. Thus, the distance can be calculated if the apparent magnitude of the host is known. The problem with this method is the difficulty of the host galaxy detection. Contamination by DC white dwarfs, faint stars with a similar featureless spectrum, is a problem for optical BLO samples. Optical samples also include some radio-quiet BLO candidates (up to 86 in Plotkin et al. 2009). However, confirmed cases do not exist yet, and it would indeed be difficult to explain the lack of radio emission from an AGN with jets.

Currently, new BLO samples are discovered principally by cross-correlating existing survey catalogues, mainly at radio and X-ray wavelengths, and performing follow-up optical spectroscopy on the candidate sources to ascertain the expected lack of strong emission lines (Perlman et al. 1998, Turriziani et al. 2007, Plotkin et al. 2008). The first-step candidate selection is most often based on applying constraints on the broad band spectral indices of the sources, or requiring a flat radio spectrum ($\alpha \leq 0.5$, $S \propto \nu^{-\alpha}$). Thus, BLOs are at present selected based on their broad band emission properties and the featureless spectrum, while the variability behaviour and the degree of polarization of the new members of the class are often unknown due to lack of data. This has slowly lead to a very inhomogeneous BLO population. For example, whereas the very first BLOs exhibited, by definition, strong variability in radio frequencies, the newer BLOs can have a single low radio frequency datapoint, from which the required radio-optical broad band spectral index can be determined. The inhomogeneity of the class has also warranted the further subdivision of the population according to different schemes (discussed in more detail in Sect. 4), as well as instigated the need of exploring the properties of the population in a consistent way using large samples including all possible BLOs.

Another property of BLOs, the use of which has evolved during the decades, is their energy distributions. Strittmatter et al. (1972) formulated that BLOs should emit most of their energy in the infrared (IR) frequencies. The BLO population today is far more diverse; the peak of the energy emission can be anywhere from radio to X-ray wavelengths. As we shall see in the following sections, exploring this wide range of BLO emission and its causes is the cornerstone of this dissertation.

2.3.2 Flat-spectrum radio quasars and their difference from BLOs

Flat-spectrum radio quasars (FSRQs) are similar to BLOs. They, too, are beamed and variable, but FSRQs typically exhibit strong emission lines in their optical spectra unlike BLOs (see the top panel of Fig. 2.6). FSRQs can further be divided into subclasses such

as optically violently variable (OVV) quasars, high-polarized quasars (HPQ) and low-polarized quasars (LPQ). OVV quasars are extremely variable at optical wavelengths in short time scales. OVVs are also highly polarized. Nowadays they are rarely discussed as a class, but rather pooled together with other FSRQ. The dividing line in the degree of polarization, P_{pol}, between HPQ and LPQ is taken to be 3 %. The division is not very robust, however, because the degree of polarization can also vary and just one $P_{pol} \geq 3\,\%$ measurement is enough for an HPQ classification.

Although so similar, there are some differences between BLOs and FSRQs besides optical spectra. Firstly, FSRQs have significantly higher redshifts than BLOs. In the Roma-BZCAT blazar catalogue (Massaro et al. 2009) the average redshift for FSRQs is $z = 1.41 \pm 0.79$, while for BLOs $z = 0.34 \pm 0.22$. Due to weak or missing emission lines almost half of the BLO population is lacking an accurate redshift measurement, but this fact alone is not sufficient in explaining the dissimilar distributions.

In the unifying scenarios for AGN types, BLOs and FSRQs are usually annexed to different parent populations. BLOs are identified as the beamed counterparts of FRI radio galaxies, while FSRQs correspond to FRII radio galaxies. Lately it has become apparent that the division is not so straightforward (Landt & Bignall 2008). FRI's have no or very weak emission lines and FRII's typically are strong-lined (Zirbel & Baum 1995), but a minority of FRII's also have featureless spectra. Thus, they are easily classified as BLOs, making their parent population heterogeneous.

The results of the Fermi Gamma Ray Space Telescope have revealed another difference between BLOs and FSRQs. The gamma ray spectra of BLOs are considerably harder than those of FSRQs (Abdo et al. 2009). Ghisellini et al. (2009) also found that FSRQs are more luminous in the gamma-ray region. They suggested that both these properties, as well as the strength of the emission lines, are governed by accretion. In their scenario, below a critical accretion rate, the disk becomes radiatively inefficient and the ionizing flux weakens, resulting in weak emission lines. Because of the weak disk, there is little external radiation in the medium. Thus, the jet does not suffer much cooling and the radiation reaches very high energies producing harder spectra. The result is a BL Lac object. In the opposite end is a system with an efficient accretion disk, producing strong emission lines and a sufficiently strong external radiation field to cool the jet electrons so that they only reach moderate energies. This we observe as an FSRQ.

3 Energy distributions of blazars

3.1 Radiation mechanisms

All radiation we see from AGN and other celestial objects has its origins in the workings of atomic and subatomic particles. Electromagnetic emission can be divided into two parts: thermal and non-thermal radiation. In keeping with its name, thermal radiation is produced due to the temperature of the source. Typically, it is black body radiation. Non-thermal radiation originates in other processes, such as the movement of charged particles in a magnetic field. Both kinds are produced in a blazar. However, due to the extremely strong magnetic fields present in the jets, the electromagnetic spectra of blazars are completely dominated by two non-thermal radiation components: synchrotron and inverse Compton radiation. They are discussed in more detail in the following.

3.1.1 Synchrotron emission

When electrons are accelerated in the magnetic field of the blazar jets, they produce synchrotron radiation. The electrons move in a helical path, spinning around the magnetic field lines with a gyration frequency

$$\nu_g = \frac{eB}{2\pi\gamma mc}, \tag{3.1}$$

where e and m are the charge and mass of the electron, B is the strength of the magnetic field, γ is the Lorentz factor and c is the speed of light.

In the non-relativistic case $\gamma \simeq 1$ and the process is called cyclotron radiation. When the velocity of the electron approaches the speed of light, the emitted radiation is concentrated in a narrow cone with the axis in the direction of the velocity vector and half-angle of $\theta \propto 1/\gamma$ (Fig. 3.1). Thus, the random observer in the direction of the cone would see a series of flashes of radiation at the Doppler-shifted gyration frequency ν'_g. Of course, in the case of a blazar, there is a whole population of electrons flowing in the jet. The synchrotron photons produced by a power-law population create the canonical synchrotron spectrum, shown as the lower frequency bump in Fig. 3.2. At low frequencies the spectrum is self-absorbed, i.e., the electron population absorbs a part of the synchrotron photon population it has produced. When this happens, the source is said to be optically thick as most of the photons cannot escape without being reprocessed. This synchrotron self-absorption process gives the low-frequency end of the spectrum a spectral index of 5/2. After the turnover, the source is optically thin and the spectrum falls as $S(\nu) \propto \nu^{-\alpha}$. If the electron population producing the synchrotron radiation has a power-law energy distribution $dN/dE \propto E^{-s}$, then $\alpha = (s-1)/2$. In high frequencies, the spectrum gets steeper still as radiation losses limit the high frequency emission.

Synchrotron radiation is always polarized. Emission from a single electron is elliptically polarized, but due to geometrical effects, the elliptical components cancel each other out and the radiation we observe is partially linearly polarized.

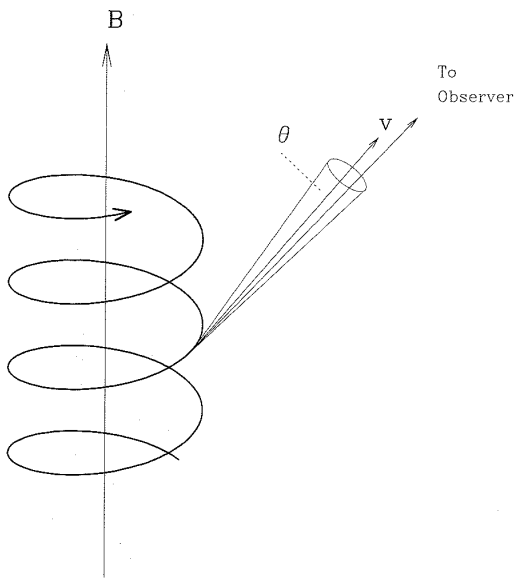

Figure 3.1: Relativistic electrons move in helical path in a magnetic field and emit synchrotron radiation in a narrow cone of opening angle θ. (Kembhavi & Narlikar 1999)

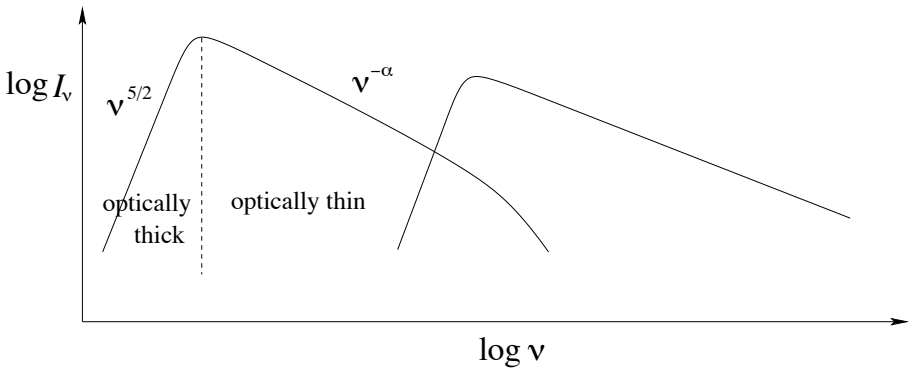

Figure 3.2: The spectrum of the synchrotron radiation (low frequency bump) and Inverse Compton radiation (high frequency bump). The optically thick region of the synchrotron component has a spectral index of 5/2, while the optically thin side has a negative index which is dependent on the energy distribution of the electron population producing the radiation. The Inverse Compton component, assuming SSC, follows the shape of the synchrotron component.

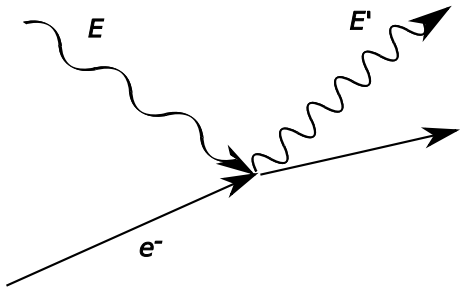

Figure 3.3: A diagram of inverse Compton scattering. The relativistic electron collides with the photon, boosting it to a higher energy E'.

3.1.2 Inverse Compton emission

Another radiation mechanism essential to blazars is Inverse Compton (IC) emission, or Inverse Compton scattering. Regular Compton scattering occurs when a photon collides with a particle at rest, loses some of its energy, and is shifted to longer wavelengths. Conversely, in IC scattering photons gain energy from collision with moving electrons (Fig. 3.3). It can be shown that the energy of an IC scattered photon is $E' = \gamma^2 E$, where E is the energy of the incident photon and γ is the Lorentz factor of the electron. This applies only when the incident photon energy is $E < mc^2/\gamma$, and, thus, the fraction of energy lost by the electron in the collision is $\ll 1$ (Kembhavi & Narlikar 1999).

IC radiation requires a dense photon field, which implies a compact, luminous source, such as a blazar. The origin of the seed photons that are scattered is a topic of much debate. The synchrotron self-Compton (SSC) model is a strong candidate (Bloom & Marscher 1996). In SSC, electrons scatter their own synchrotron photons. Fig. 3.2 depicts the IC spectrum when SSC is assumed. Relativistic electrons have two channels of losing their energy in a blazar jet: synchrotron radiation and upscattering photons via IC process. The ratio of the power of these two processes is

$$\frac{P_C}{P_s} = \frac{U_{ph}}{U_B}, \tag{3.2}$$

where U_{ph} is the energy density of the photons and U_B that of the magnetic field. Eq. 3.2 shows that if the energy density of the photons is initially larger than U_B, it will remain so as the photons undergo multiple scatterings, as long as the electrons exhaust their energy and the source is quenched. This is called the Compton catastrophe. It limits the theoretical brightness temperature of compact, optically thick sources to $\leq 10^{12}$K (Kellermann & Pauliny-Toth 1969). It has been showed by Readhead (1994), however, that AGN seem to keep their brightness temperatures well below that point, at about 10^{11}K. In their scenario, an unknown physical mechanism favours the equipartition of energy between the photon and magnetic fields. For now, it remains unclear whether the equipartition requirement is enough to limit the brightness temperatures of AGN to 10^{11}K (Tsang & Kirk 2007).

Besides SSC, the seed photons for IC process can come from an external radiation field. This is called external inverse Compton (EIC). The photons could originate in the accretion disk and be intercepted by the jet directly, or after being scattered by the BLR (Dermer & Schlickeiser 1993, Sikora et al. 1994, Dermer et al. 2009). Alternatively, the infrared emission of the dusty torus can produce the seed photons (Błażejowski et al. 2000). The nature of the IC radiation depends on the location of the emitting region in the jet; if it is located beyond the torus, then SSC will probably dominate, whereas closer to the central engine EIC will be more prominent (Sokolov & Marscher 2005). In any blazar, both processes are likely to contribute. It has also been suggested that the high-energy emission of BLOs would be principally of the SSC kind, while that of the FSRQs would be mostly EIC (Sikora et al. 1994, Ghisellini et al. 1998). This will be discussed more in Sect. 4.

3.2 The shape of the spectral energy distributions of blazars

The continuum spectra of astronomical objects are usually presented in the form $\log S$ vs. $\log \nu$. In the spectral energy distribution (SED), the flux density is multiplied by frequency, i.e., the spectrum in presented as $\log \nu S$ vs. $\log \nu$. The reason for the popularity of the SED presentation of spectra is briefly quantified below (following the treatment by Kembhavi & Narlikar (1999)).

The dependence between the flux density, or luminosity L, and frequency ν of AGN can be approximated with a power law

$$L(\nu) = A\nu^{-\alpha}, \tag{3.3}$$

where A and α are constants. Thus, the integrated luminosity radiated between two frequencies ν_1 and ν_2 is given by

$$L(\nu_1, \nu_2) = \frac{A}{1-\alpha}(\nu_2^{1-\alpha} - \nu_1^{1-\alpha}), \quad \alpha \neq 1, \tag{3.4}$$

or

$$L(\nu_1, \nu_2) = A \log \frac{\nu_2}{\nu_1}, \quad \alpha = 1. \tag{3.5}$$

To determine how much luminosity is radiated for every logarithmic interval of frequency, i.e., the interval $\Delta \log \nu = 1$, we can use Eqs. 3.3 and 3.5 on a frequency interval $(\nu, 10\nu)$ and obtain

$$L(\nu, 10\nu) = A = \nu L(\nu). \tag{3.6}$$

Strictly this applies only when $\alpha = 1$, but is a reasonably good approximation also for $\alpha \neq 1$ spectra.

Thus, every point in the SED tells us how much energy is emitted in the next logarithmic interval from that particular frequency. The basic $\log S$ vs. $\log \nu$ -spectra are often quite steep as the flux densities decline rapidly towards the higher frequencies. At the same time, however, the bandwidth per logarithmic frequency interval increases. As a result, the SED does not decline nearly as rapidly. As we see from Eq. 3.6, when $\alpha = 1$,

the SED is constant and features no slope at all. Fig. 3.4 describes the differences between the two representations of spectra. It is noteworthy that the relation between the spectral indices, i.e., the slopes, is $\alpha_{SED} = \alpha + 1$.

The SED representation shows at a glance where the bulk of the energy from the source is emitted. In the case of blazars, the SED has a characteristic shape of two bumps. The first is assigned to synchrotron radiation and the second is due to IC scattering. As mentioned, these are both non-thermal processes, dominating because of the strong Doppler boosting of the source. In unbeamed, normal quasars, also the thermal emission from the accretion disk can be discerned as a feature in the optical/UV region called the big blue bump (Malkan & Sargent 1982, Shang et al. 2005). Lately, signs of the accretion disk radiation have also been found in blazars (Pian et al. 1999, for a good review on the matter see Perlman et al. (2008)). Investigating thermal emission might shed light especially on the reason behind the different emission features of BLOs and FSRQs. However, for the purposes of this dissertation, the blazar SED can be thought of as two bumps which can be modelled with smooth curves.

In Paper I and Paper IV we fitted the synchrotron components of blazar SEDs with a parabolic function. Using the largest sample to date, 398 sources, we were able to establish the range of the synchrotron peak frequency variability in BLOs (Paper I). The distribution of peak frequencies, ν_p, was relatively smooth across the range of 12.67 – 21.46. The interval $\log \nu_p = 13 - 14$, where the peak falls into the IR region, was the most populated. For 22 sources in total $\log \nu_p > 19$, which is exceptionally high. Although at least for some of these sources the peak frequency is overestimated due to sparse data, there could be sources whose synchrotron peak extends all the way to the MeV -region (Ghisellini 1999, Beckmann 2003). So far, however, these extreme HBLs have gone undetected, and it would require additional data to ascertain the extreme nature of the high ν_p sources in Paper I. In Paper IV the range of ν_p was much narrower, because the sample includes only radio-bright sources. The distribution of Doppler-corrected synchrotron peak frequencies peaks in the interval $\log \nu_p = 12 - 12.5$, i.e., in the far-infrared domain.

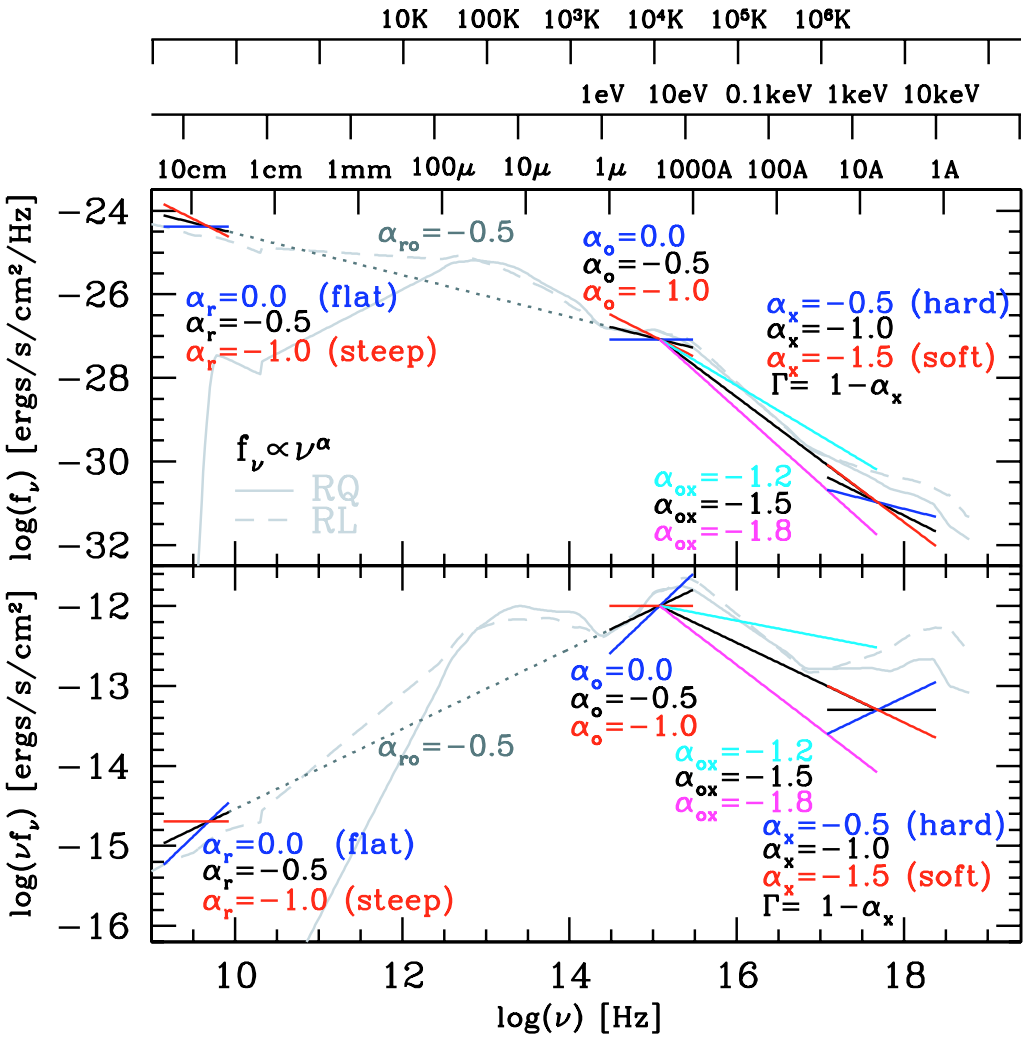

Figure 3.4: The two representations of AGN emission: a normal log-log spectrum (top) and a spectral energy distribution of the same source (bottom). The range of different spectral indices is also presented for comparison. The underlying spectra are typical spectra for radio loud and radio quiet normal quasars. They feature slightly different components because of notable host galaxy emission. However, the radio to optical spectrum of radio loud quasars is very similar to that of blazars. (Richards et al. 2006)

4 Blazar sequence

Early on, it was noticed that BLOs had different characteristics depending on the wavelength region of the survey in which they were found. Radio-selected objects (RBLs) are on average more luminous, variable, and polarized, and their structure is more core-dominated than that of X-ray-selected objects (XBLs) (Perlman & Stocke 1993, Jannuzi et al. 1994). XBLs also have a negative cosmological evolution, which means that they are more abundant at low redshifts (Morris et al. 1991, Wolter et al. 1994). There also is a clear dichotomy in the distributions of the ratio of X-ray and radio fluxes, the dividing line being $\log S_X/S_r = -5.5$ (Padovani & Giommi 1995, Brinkmann et al. 1996). At first, the differences in the properties were assigned to different viewing angles. The radio jet was thought to be more collimated than the X-ray jet, and RBLs were thought to be seen at smaller viewing angles than XBLs (Urry & Padovani 1995).

RBLs and XBLs also occupy different regions in the $\alpha_{ro} - \alpha_{ox}$ -plane (Ledden & Odell 1985). This indicates differences in their multifrequency emission. Giommi & Padovani (1994) and Giommi et al. (1995) suggested that the fundamental difference between RBLs and XBLs was in their SEDs; RBLs had a cutoff in the IR energies, whereas that of XBLs reached the optical or UV, or even X-ray frequencies. The selection band nomenclature was soon replaced by the more physical names of low-energy BL Lacs (LBLs) and high-energy BL Lacs (HBLs) (Padovani & Giommi 1995).

Laurent-Muehleisen et al. (1999) and Bondi et al. (2001) found the first samples of BLOs with properties intermediate between RBLs and XBLs. Accordingly, these sources are dubbed intermediate BL Lacs (IBLs). They fall nicely between RBLs and XBLs in the spectral index distributions, and they bridge the gap in the $\log S_X/S_r$ distributions. Thus, from a divided population, we arrive at a continuous distribution of BLOs. The greatest distinction between the sources is the frequency at which the peak of their synchrotron emission lies, and LBLs and HBLs represent the extremes of this continuum.

The spectral sequence of BLOs, combined with some FSRQs, was first connected to bolometric luminosity by Sambruna et al. (1996). They derived the synchrotron spectra for a sample of blazars and studied the broadband spectral indices and their relationship to other properties, such as luminosity and redshift. Fossati et al. (1997) and Fossati et al. (1998) developed the idea further and it soon became known as the blazar sequence. It has the following observational characteristics (Fossati et al. 1998):

- Blazar SEDs have two peaks (synchrotron and IC), the first of which is anticorrelated with source luminosity
- The X-ray spectrum becomes harder and γ-ray spectrum softens with increasing luminosity, indicating the luminosity-related movement of the second peak as well
- Therefore, the ratio of the frequencies of the two peaks is constant
- The increasing 5 GHz luminosity increases the dominance of the IC component over the synchrotron one, i.e. the ratio between the IC and synchrotron peak luminosities increases (this is known as Compton dominance).

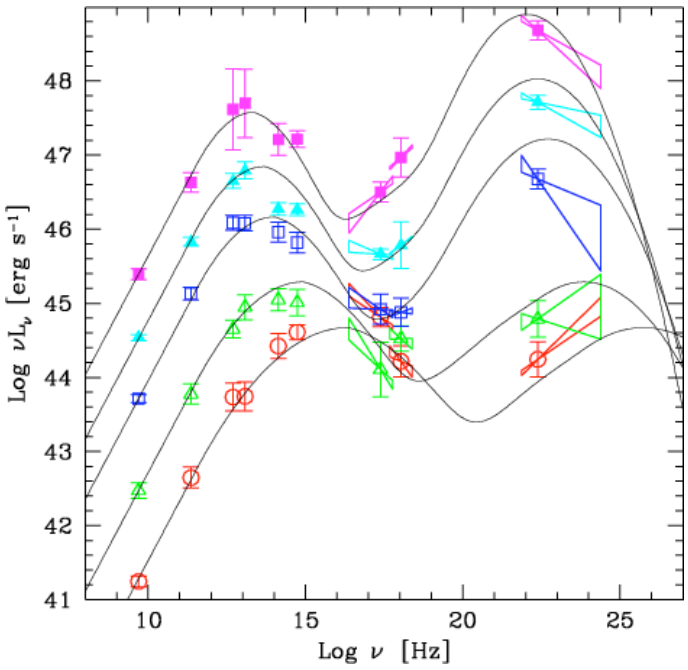

Figure 4.1: Average SEDs of a sample of blazars binned according to luminosity. The first peak (roughly at frequencies $\log \nu = 13 - 16$ in the figure) is the synchrotron peak, and the second (at $\log \nu = 22 - 25$) is the IC peak. Solid lines are modelled spectra. (Donato et al. 2001)

Fig. 4.1 captures the essence of the blazar sequence scenario, depicting all the points listed above. Ghisellini et al. (1998) offered a theoretical explanation for the observations (summarized by Padovani (2007)). The energy density U of a characteristic jet can be defined by $U = L/R^2$, where L is the luminosity of the jet and R is its size. As the luminosity increases, so does the energy density, which means that the electrons undergo more collisions and cool faster. Thus, the peak electron energy, γ_{peak}, is lower. Ghisellini et al. (1998) found a connection $\gamma_{peak} \propto (U_{ph}+U_B)^{-0.6}$. As the synchrotron peak frequency ν_p depends on the electron energy as $\nu_p \propto \gamma^2_{peak}$, the result is that sources with high luminosity have lower synchrotron peak frequencies. Ghisellini et al. (1998) couple the presence of an external radiation field with source luminosity in the blazar sequence. They find that external field is unavoidable for producing emission lines and it also provides an extra source of cooling. Thus, the IC radiation is in this case at least partly of the EC kind. The theoretical principles of the blazar sequence are summarized below:

- HBLs are the least luminous sources, with a weak external radiation field and weak or absent emission lines. They suffer little cooling, and the peak of their synchrotron radiation ν_p can reach UV or X-ray frequencies.
- LBLs are more powerful with a moderate external field. Cooling is more effective, and ν_p is in the IR/optical frequencies.

- FSRQs have a strong external field, combined with the largest luminosities. Their emission lines are strong, and their synchrotron peaks are at IR region.

As the EC enhances the IC emission towards the low-ν_p -end of the range, the Compton dominance increases as well.

Despite its delightful simplicity and good correspondence with 1Jy and Einstein Slew Survey samples used by Fossati et al. (1998), the blazar sequence scenario has faced strong opposition in the last 10 years. Its main weaknesses are the limited sample of blazars it was initially based on, and the fact that the effect of Doppler boosting was not sufficiently considedred in its formulation. The first discrepancy between the blazar sequence and observations was the discovery of high-energy FSRQs, or HFSRQs. They are the strong-lined counterparts of HBLs, like "normal" FSRQs can be thought of as strong-lined counterparts of LBLs. According to the blazar sequence, strong lines and high ν_p should not co-exist in the same source, but HFSRQs were found in the Deep X-ray Radio Blazar Survey (DXRBS) (Perlman et al. 1998, Padovani et al. 2002) as well as the ROSAT All-sky Green Bank -survey (RGB) (Padovani et al. 2003). Also evidence of other inconsistent sources was found: hints of low-power low-ν_p blazars (Caccianiga & Marchã 2004) and high-power, high-ν_p BLOs (Giommi et al. 2005).

The use of larger samples to test the existence of the blazar sequence truly showed its frailty. Antón & Browne (2005) added a new radio-selected sample of blazars to the sample used by Fossati et al. (1998), weakening the anticorrelation of ν_p and 5 GHz luminosity significantly. In Paper I ν_p -values of a large sample of over 300 BLOs were determined and plotted against luminosities at several frequencies from radio to X-ray region. No correlation between ν_p and luminosity at ν_p was detected. This was mainly due to the extended distribution of the ν_p -values. In Paper I, log ν_p even reached values beyond 20. Although the most extreme values are probably exaggerated due to the parabolic function used in the SED fitting, the increased number of HBLs reveals an almost U-shaped log ν_p - log νL_{peak} -distribution.

In Paper IV we raised the question of the effect of Doppler boosting in the blazar sequence. It had not been properly studied before as most authors use a fixed value or ignore it completely. We used Doppler factors calculated from total flux density variations (Hovatta et al. 2009). The variability brightness temperature derived from modelling radio flares with an exponential function was compared with an intrinsic one. This gives a robust value of D. We also derived a new set of SEDs in a consistent manner for a sample of 135 AGN in total, including 65 blazars. These data revealed that the amount of Doppler boosting is strongly dependent on the synchrotron peak frequency, low-energy sources being more boosted. This puts the alleged blazar sequence in new light. When ν_p and νL_{peak} are corrected for Doppler boosting and their correlation re-plotted, it is evident that not only does the anticorrelation disappear, but in fact turns marginally positive. This is particularly apparent for BLOs, when the sample of Paper IV is combined with that of Paper I. This was unpredicted but fits perfectly to the number counts of BLOs, which show that HBLs are less numerous than LBLs (Padovani 2007). This fact has before been left unexplained by the blazar sequence scenario.

The effect of Doppler boosting on the blazar sequence was also considered by Wu

et al. (2007), who used the log ν_p-values derived in Paper I. They derived the core 5 GHz radio power from 408 MHz observed power with a relation found by Giovannini et al. (2001). Then the derived 5 GHz luminosity could be compared with the observed 5 GHz luminosity to get the boosting factor. They found a strong dependence between the Doppler factor D and ν_p as well. The sources with low ν_p are significantly more boosted. However, the method of Wu et al. (2007) of deriving the Doppler factors is easily affected by source variability. The 5 GHz emission of blazars is variable, and as a result, the calculated amount of boosting depends on the flux level of the source at the time.

To account for the growing evidence against the blazar sequence, Ghisellini & Tavecchio (2008) modified it and linked it with the accretion process rather than the bolometric source luminosity. They suggested that the theoretical blazar sequence is governed by the mass of the central black hole, M_{bh}, and the accretion rate $\dot{M}$. These two parameters regulate the size of the BLR ($R_{BLR} \propto \dot{M}^{1/2}$) and the distance of the site of the jet dissipation from the nucleus ($R_{diss} \propto M_{bh}$). To simplify, we get a low-ν_p SED when $R_{BLR} > R_{diss}$ and the jet dissipates inside the BLR, which provides an extra source of cooling. In the opposite case, the result is a high-ν_p SED, due to the lack of the cooling BLR photons. This scheme also allows the existence of HFSRQs. However, Ghisellini & Tavecchio (2008) make a large number of generalizing assumptions, and, as they admit, this sequence only describes the averaged blazar properties and trends. In a later paper, using the data of the Fermi Gamma-ray Space Telescope, Ghisellini et al. (2010) determine the SEDs up to the gamma-ray region. Their results support the scenario that the SED is linked to accretion, and the source luminosity is tied to the black hole mass.

The existence and form of the blazar sequence is still a matter of strong debate in blazar astronomy. While the observational evidence seems to contradict the original bolometric luminosity sequence of Fossati et al. (1998), it is clear that there is some underlying process that dictates peak frequency of the synchrotron emission. Identifying that process is a challenge for the future.

5 Radio variability of AGN

While studying the energy distributions of blazars offers a view of the steady multifrequency jet emission, variability at a single wavelength domain allows a look into the transient phenomena in the jet. Variability at radio frequencies is the other focus of this dissertation.

5.1 Shock model

The flux density variability of AGN has for a long time been attributed to shocks moving in the jet flow. This concept was first presented by Blandford & Königl (1979), and further developed by Marscher & Gear (1985). A shock can be seen travelling in the jet in Fig. 2.2. The shock model was developed to improve on the expanding cloud model (van der Laan 1966, Pauliny-Toth & Kellermann 1966), in which quasar variability was assigned to a symmetrical optically thick synchrotron source expanding in a magnetic field. In the shock model, a disturbance, i.e., shock, is travelling along the jet. In the shocked region, the magnetic field is compressed, and the plasma flowing in the jet is accelerated beyond its normal speed Γ. (Here Γ is used to refer to the Lorentz factor of the bulk flow, whereas γ denotes the Lorentz factor of a single particle.) Thus, the radiation emitted by the plasma intensifies, which we observe as a sudden rise in the flux density of the source. The shocks can often be seen propagating in the jet flow with very long baseline interferometry (VLBI). In that context, they are also known as superluminal knots, because their apparent speeds can exceed the speed of light manyfold.

In the Marscher & Gear model, the electrons are accelerated in a very narrow area in the shock front. This is also the site of high-frequency radio emission. As the accelerated electrons gain distance from the shock front, they suffer radiative losses, and the frequency of their emitted radiation gets lower. Thus, there is a gradient in the frequency of the radiation emitted by the accelerated electrons perpendicular to the shock front. The closer to the shock, the more energetic the emission. This is called local frequency stratification (Marscher 2009). As a result, the time scales of high-frequency variability are characteristically shorter, because the emission is originating in a smaller area. Frequency stratification also creates time delays between the wavebands.

The spectrum of the shock emission has the shape of that of a synchrotron source. The Marscher & Gear model predicts the time evolution of the spectrum, which is simplified in the general shock model of Valtaoja et al. (1992):

- Compton (growth) stage: the peak of the shock spectrum, ν_m, moves to lower frequencies and the peak flux, S_m, increases. At this stage, the electrons cool primarily through Compton losses.
- synchrotron (plateau) stage: S_m is constant as ν_m continues to decrease. Radiation density decreases and the plasma cools via synchrotron process.
- adiabatic (decay) stage: the shock region expands and cools adiabatically and S_m decreases along with ν_m as the shock decays.

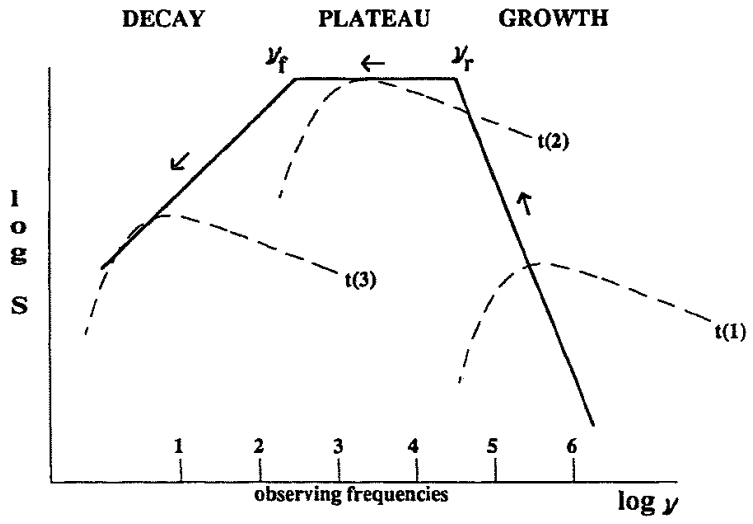

Figure 5.1: The temporal evolution of the spectrum of the shocked region. The dashed curve is the shock spectrum, the thick line represents the track its peak makes in the log S - log ν -plane. (Valtaoja et al. 1992)

The temporal evolution is depicted in Fig. 5.1. In the terminology used by Valtaoja et al. (1992), the flare is high-peaking if it reaches its peak flux density at frequencies higher than the observing frequency and low-peaking if the flare peaks at frequencies lower than the observing frequency ($\nu_{obs} < \nu_f$ and $\nu_{obs} > \nu_r$ in Fig. 5.1, respectively). High- and low-peaking flares have slightly different characteristics. The easiest to study from radio flux curves are the maximum flux density and possible time lags between the flux peaks in different frequencies. In high-peaking flares the peak flux decreases from one frequency to the next, and the maxima are increasingly time-delayed. In low-peaking flares there are no time lags and the maximum flux density is still increasing.

AGN variability has been explained by other means as well. A popular alternative to the shock model is the helical jet model connected to binary black hole systems (e.g., Conway & Wrobel 1995, Villata & Raiteri 1999, Ostorero et al. 2004). The main idea is that the orbital or precession motion of the central engine causes the twisting motion of the jet. Different emission sites of the inhomogeneous jet meet the line of sight in turn and are additionally boosted, so that high-frequency emission is leading. This way the observational signatures would look very much like those of the shock model. The problem with helical jet models is the periodicity, which is expected as a result of the orbital motions of the binary black hole. Thus far, the behaviour of the modelled sources has not complied to the helical jet framework (Raiteri et al. 2006).

The binary black hole system has also been suggested to explain the periodical optical variability of the BL Lac object OJ 287 (Sillanpää et al. 1988, Lehto & Valtonen 1996), but in slightly different manner. The flares would not be caused by a helical jet, but the

tidal interactions on the accretion disk of one or both of the black holes at periastron. In the Lehto & Valtonen model the secondary black hole plunges through the accretion disk of the primary, causing a flare as it emerges on the other side. Valtaoja et al. (2000) modified the model to explain also the radio flaring. However, also these models have run into some trouble with the unpredictable behaviour of the source (Kidger 2000, Valtonen et al. 2008), although modifying the model has helped in reproducing the observed light curve (Valtonen et al. 2009).

5.2 Long-term monitoring

When studying highly variable objects, such as blazars, it is clear that a single radio flux measurement reveals very little about the source emission in general. To really get an idea of the typical flux levels and the amplitude of variability we need constant monitoring that goes on for decades or longer, which still is a blink of an eye compared to a blazar's lifetime.

There are currently two ongoing AGN monitoring programmes in the radio frequencies. Metsähovi Radio Observatory in Finland monitors the northern sky at 22 and 37 GHz. They use a 13.7-meter parabolic antenna and the flux curves date back to 1980's. Metsähovi observes roughly 100 brightest sources approximately once a month. The data have been released in several publications (Salonen et al. 1987, Teräsranta et al. 1992, 1998, 2004, 2005, Paper II). Fig. 5.2 shows the flux curve of BL Lacertae at 37 GHz as an example of a typical, very variable and bright blazar. It has been monitored in Metsähovi since 1979. In the early 80's it had the strongest flare to date, and since then there has been several outbursts with short intervals.

The other radio monitoring programme is maintained by the University of Michigan Radio Astronomy Observatory (UMRAO). They observe at 4.8, 8 and 14.5 GHz with a 26-meter antenna. They started the monitoring as early as 1960's, and many of their monitored sources are also in the Metsähovi source list. Together the Metsähovi and UMRAO programmes offer a wealth of data and quite extensive coverage of the cm and mm-wavelengths. This kind of monitoring programmes are the only tool that allows us to put some limits on the typical AGN variability. However, it should be remembered that those limits can never be constant; AGN can change their variability behaviour unexpectedly, and even in a certain subgroup individual sources can behave very differently.

5.3 Variability characteristics

Putting it simply, the observational propeties of AGN flares are defined by three dimensions: flux density (what is the flare amplitude?), time (how long does it last, how often do they occur?) and frequency evolution (how does the flare develop from one frequency to the next?). In the following, flares will be discussed from these three viewpoints.

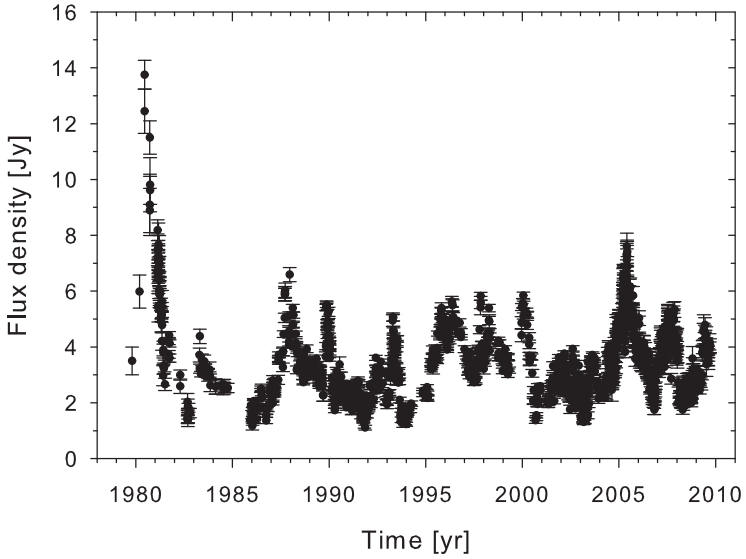

Figure 5.2: The 37 GHz flux curve of the blazar archetype, BL Lacertae. Data are from Metsähovi Radio Observatory.

5.3.1 Flux density

The amplitude of the flux variations of blazars and other AGN can be quite large, even tens of Janskys in the most extreme sources. To make the absolute flux density values comparable when quantifying the variability in individual sources, it is customary to use a variability index, defined as

$$V_{varI} = \frac{(S_{max} - \sigma_{S_{max}}) - (S_{min} + \sigma_{S_{min}})}{(S_{max} - \sigma_{S_{max}}) + (S_{min} + \sigma_{S_{min}})}, \tag{5.1}$$

or sometimes simply

$$V_{varII} = \frac{S_{max} - S_{min}}{S_{min}}. \tag{5.2}$$

In both equations, S_{max} and S_{min} are the maximum and minimum flux densities of the source, respectively, and $\sigma_{S_{max}}$ and $\sigma_{S_{min}}$ their errors. Another way to quantify variability is to use the index

$$F_{var} = \frac{1}{\langle S \rangle} \sqrt{X^2 - \langle \sigma_{err}^2 \rangle}, \tag{5.3}$$

where $\langle S \rangle$ is the mean flux, X is the total variance of the light curve and σ_{err}^2 is the mean error squared (Edelson et al. 2002). Variability indices help in comparing the variability amplitudes of AGN subgroups. This has been done in Paper III in all Metsähovi and UMRAO frequency bands. We found that the variability indices at 4.8 GHz were significantly lower than in other frequencies. This is understandable, because at the beginning of the

flare the 4.8 GHz emission is mostly self-absorbed, and intensifies in the decay stage of the shock. Also, due to frequency stratification, flares in low frequencies last longer, and often the shock components of different outbursts are blended and diluted. A similar conclusion was also reached by Soldi et al. (2008), who calculated the F_{var} for 3C 273 at several wavelengths. The F_{var} vs. ν -spectrum had a sharp rise from radio to sub-mm region, indicating a lower variability amplitude at low radio frequencies.

In Paper II we report the results of an extensive BLO observing campaign. A large sample of 398 BLOs including many faint sources with little or no radio data was observed in Metsähovi beginning 2001. This was a unique opportunity to establish the radio flux levels of the BLO population. The majority of BLOs, especially HBLs, are expected to be faint, but real evidence of their long-term behaviour has been lacking. This knowledge is also important in the image reduction of the Planck satellite, which was launched in May 2009. Planck is mapping the cosmic microwave background radiation (CMB). To achieve the best possible quality in the maps, the radiation of the foreground sources must be taken into account in the data processing. This requires direct obsevational information about the expected flux levels of the foreground sources.

The results of Paper II show that most BLOs are indeed very faint at 37 GHz. Only 35 % of the BLO sample was detected at Metsähovi at $S/N > 4$ level. With the Metsähovi observing equipment, the detection limit ranges from 0.2 to 0.6 Jy depending on the weather conditions. As much as 86 % of HBLs went undetected during the whole 3.5 -year campaign. A large majority of the detected sources has an average flux below 1 Jy at 37 GHz. Interestingly, our findings in Paper II suggest that even the faintest of BLOs may undergo flaring similar to brighter sources. There were many faint sources which had several non-detections and one or two measurements clearly above the detection limit. Also, many high-energy sources which had only one detection at 37 GHz exhibit a clearly inverted spectrum between 5 and 37 GHz. This indicates that the 37 GHz measurement may have been taken at a particularly bright state. If their spectra in quiescence resembles the average BLO spectrum, their 37 GHz quiescent flux should be of the order of 50 mJy or less. Thus, to reach the detection limit, they have to increase their flux levels substantially.

BLOs are generally thought to be more variable than other AGN, which is corroborated by Aller et al. (1999) and Paper III. For example, for BLOs $\tilde{V}_{varI} = 0.78$ and for other quasars $\tilde{V}_{varI} = 0.68$ at 37 GHz (Paper III). The value of V_{varI} is, however, extremely sample-dependent. In most variability studies, the sample contains sources that are already known to be variable, and, as such, interesting. In Paper II where we used the whole Metsähovi BLO sample, $\tilde{V}_{varI} = 0.3$. It is also noteworthy that the median variability indices of LBLs and HBLs were not very different, $\tilde{V}_{varI} = 0.32$ and $\tilde{V}_{varI} = 0.30$ respectively. Thus, our study lends no direct support to claims of stronger average variability of LBLs. It has to remembered, however, that the majority of faint HBLs go undetected at 37 GHz. Also, the variability indices are heavily influenced by the length of the monitoring period and the number of measurements. The 3.5 -year monitoring of Paper II is not enough to reveal any characteristic behaviour patterns in individual sources, even though it is long enough for determining the average flux levels of the population.

The variability indices are calculated with all-time minimum and maximum fluxes,

and do not represent the amplitudes of individual flares. The calculation of a flare amplitude is tricky, because due to overlapping shock components the time of the flare onset is difficult to determine from the flux curves, even if the sampling is dense. The range of typical flare peak fluxes is diverse. In Paper V, the smallest BLO flare peak flux density was 0.7 Jy, while the maximum was 12.1 Jy. The highest flux level for a blazar during the whole Metsähovi monitoring programme, 56.7 Jy, was reached by the low-polarized quasar 3C 273 in 1991 (Paper III).

5.3.2 Time scales

The occurence, the duration, and the possible periodicity are probably the most studied aspects of AGN outbursts. The flux curves represent a typical time series and for those we have well-developed tools, such as the structure function (SF) (Simonetti et al. 1985), the discrete correlation function (DCF) (Edelson & Krolik 1988, Hufnagel & Bregman 1992) and the periodogram (Lomb 1976, Scargle 1982). The structure function gives usually a shorter time scale, which corresponds to the rise and decay times of flares, whereas the DCF and periodogram provide the peak-to-peak time scale of major flares. They all have been used on AGN flux curves. Hughes et al. (1992) calculated the structure functions from UMRAO data, obtaining mean time scales of 1.95 and 2.35 years, for BLOs and quasars respectively. Periodicities in UMRAO data were searched for by Aller et al. (2003), but none were found. Metsähovi data has been analyzed by Lainela & Valtaoja (1993), and more recently, by Hovatta et al. (2007). The latter made an extensive analysis of both UMRAO and Metsähovi data up to 2005, as well as some mm – data, using all three methods, the SF, DCF and periodogram. They found that the time scales of AGN classes are remarkably similar, and no significant differences between the subgroups were revealed. For example, at 37 GHz, the mean DCF time scale was 4.2 years.

The UMRAO and Metsähovi databases have also been analyzed with the wavelet method (Kelly et al. 2003, Hovatta et al. 2008). The wavelet analysis has the advantage of providing also the temporal evolution of the acquired time scale. For instance, Hovatta et al. (2008) found that few of the characteristic time scales persisted throughout the monitoring period, and only in eight sources the time scale could be detected in other frequency bands. Average characteristic time scale for flare duration was found to be 1.03 years at 37 GHz. Kelly et al. (2003) used wavelets to find quasiperiodicities for roughly half of the UMRAO sample. The sources had an average characteristic time scale of 2.4 ± 1.3 years.

In Paper III and Paper V we studied the observational flare characteristics determined directly from the flux curves. With a simple visual inspection, both studies concluded that the average flare duration is approximately 2.5 years, for both BLOs (Paper V) and other AGN (Paper III). Of course, scatter is enormous as the longest BLO flare determined in Paper V lasted for 13.2 years, while the fastest was over in 6 months. Again, this testifies to the diverse variability behaviour of AGN. The average value agrees, within reason, with the results obtained by Hovatta et al. (2008) and Kelly et al. (2003), as well as with those of Hughes et al. (1992) and Hovatta et al. (2007), when we remember that the SF time scale is linked to the rise and decay times of the flares. Paper V concludes that the

computational time scales and the flare parameters extracted visually from the flux curves have a reasonably good cor respondence, although scatter in their correlation is large.

In summary, the AGN flare time scales are source-dependent. The flux curve morphology varies from fast and frequent outbursts to decade-long flares with slow rises and decays. On average, a flare lasts for 2 to 3 years. Although periodicities are much sought after and sometimes claimed (e.g. Raiteri et al. 2001, Ciaramella et al. 2004), so far no AGN has exhibited well-documented, predictable radio outbursts. It is also noteworthy that, according to Paper III and Paper V, the Doppler-corrected luminosity has no relation to the duration of the flare, that is, longer flares are not brighter than shorter ones.

5.3.3 Frequency evolution

Tracking the evolution of the radio flare from frequency to frequency is extremely difficult due to varying sampling and the ambiguous definition of the flare. To really test the shock model, we would need to separate the often overlapping shock components and follow their development through the frequency space. With the current monitoring data, this is extremely difficult, and sometimes impossible. In Paper III and Paper V we followed the development of the flares in the UMRAO and Metsähovi frequencies. We treated the flares as periods of heightened activity rather than individual shocks, their beginnings and ends determined from the flux curves. We studied the order in which the flare reached each frequency, and the order in which the peak flux density decreased. Both papers reached the same conclusion: AGN flares adhere well to the generalized shock model. Most of the flares were high-peaking, i.e., the high radio frequencies peak first and the peak flux density decreases with decreasing frequency. The specific time lags are harder to define. It would require very dense sampling to get any meaningful results. Time lags are calculated in Paper III for as many sources as possible, and plotting them against the normalized frequency yields more evidence in support of the shock model.

Stevens et al. (1994) analyzed the behaviour of blazar flares between 22 and 375 GHz. Also in these higher energies, the frequency evolution follows the shock model. They found also examples of low-peaking flares and flares in their plateau stages (as defined in Fig. 5.1). They concluded that blazar flares probably reach their maximum development at 90 GHz or below. This is quite well in accordance with our findings of AGN flares being high-peaking at UMRAO and Metsähovi frequencies. Pyatunina et al. (2006, 2007) modelled the radio flares of 7 blazars, all of which are monitored in Metsähovi and UMRAO. They used Gaussian fits and calculated the time delays from the fit peaks. All sources showed clear frequency-dependent time delays in accordance with the shock model. Detailed studies of shock evolution have been presented for 3C 273 (Türler et al. 1999, 2000) and 3C 279 (Lindfors et al. 2006). They use the same method of fitting the radio to sub-mm (3C 273) or optical (3 C 279) flux curves with an empirical, analytical function, and also find the outbursts to adhere to the shock model for the most part. Unfortunately, the flux curves allowing this kind of modelling are available only for very few sources.

6 Conclusions

This thesis deals with the synchrotron emission of blazar jets, giving a multifrequency view in the form of the spectral energy distributions and investigating the transient phenomena in the form of radio variability. The goal of the research was to gain knowledge about these aspects of the heterogeneous blazar population using consistent methods on large, unlimited samples. The main findings can be condensed in these three points:

1. The BLO population is continuous. In the past the different discovery techniques of BLOs led to two different subgroups, RBLs and XBLs. The existence of intermediate objects slowly became apparent (Laurent-Muehleisen et al. 1999, Bondi et al. 2001). Our study of SEDs (Paper I) was the first to establish the continuous distribution of synchrotron peak frequencies ν_p with a large sample of hundreds of sources. Our radio observations of the same sample of BLOs reach the same conclusion (Paper II): there is no clustering among the detected BLOs when their 37 GHz flux levels are considered. While the flux densities certainly differ, their distribution is smooth. The same is true also for the level of variability observed among the population.

2. The term "blazar" encompasses sources with an exceptionally wide range of properties. All publications included in this thesis testify to this same conclusion. The radio luminosity of blazars can range up to 5 magnitudes at 37 GHz, and their synchrotron peak frequencies up to 7 magnitudes (Paper I) or even more depending on the existence of the extreme HBLs. As a contrast to the radio-bright objects, there is a multitude of BLOs below the detection limit at 37 GHz. However, they cannot be considered as radio-silent due to the spurious detections obtained in the Metsähovi observing campaign (Paper II). Even among the radio-bright blazars there is no preferred mode of variability (Paper III, Paper V). For example, the flare amplitudes vary from 1 to 10 Jy and the flare duration from 0.5 to 13 years for BLOs, approximately. From the literature we know that emission features can either be distinct (FSRQs) or nonexistent (BLOs), or anything in between. Thus, we classify under the same title sources with bright and variable radio emission, synchrotron peak in the IR domain, and prominent emission lines and sources with faint radio flux, synchrotron peak in the X-rays, and featureless spectra. The only discontinuity in the unified blazar population seems to be in their redshifts (Abdo et al. 2009, Massaro et al. 2009). BLOs and FSRQs differ also in their gamma-ray emission properties (Abdo et al. 2009, Ghisellini et al. 2009), but their summed distribution tends to be smooth. When the redshifts are concerned, however, this does not seem to be the case. One of the most intriguing questions for future work is whether there is a fundamental difference between LBLs and FSRQs, or should they be considered as a uniform group of low-energy blazars.

3. The blazar sequence in its original form does not exist. A defining feature in the original blazar sequence was the anticorrelation of synchrotron peak frequency and synchrotron peak luminosity. Our research with a large sample of BLOs concludes that

this anticorrelation does not exist (Paper I). In Paper IV the same conclusion is drawn when the Doppler-corrected values are used for the first time. Thus, the original blazar sequence appears to be an artefact of Doppler boosting. The Doppler correction actually turns the ν_p- L_p –correlation positive. The positive correlation is very clear, especially for BLOs, and beckons further investigation. The synchrotron peak frequency is indicative of the jet power, which is generally accepted to be of the same order than the accretion rate $\dot{M}$ (Rawlings & Saunders 1991, Allen et al. 2006, Sambruna et al. 2006). In this case it implies that the accretion rates of HBL would be higher than those of LBLs. This directly contradicts also the renewed blazar sequence (Ghisellini & Tavecchio 2008) according to which low-energy objects accrete more efficiently than high-energy objects. The dependence between ν_p and Doppler boosting factor is remarkable as well. The boosting factor is defined by the Lorentz factor and viewing angle, and preliminary results indicate that the viewing angle correlates with ν_p. High-energy blazars are seen from a larger angle than low-energy ones. The implications are a topic of future research.

7 Summary of the papers

7.1 Blazar spectral energy distributions

Paper I: *Spectral energy distributions of a large sample of BL Lacertae objects*
by **Nieppola, E.**, Tornikoski, M. and Valtaoja, E.
Paper IV: *Blazar sequence - an artefact of Doppler boosting*
by **Nieppola, E.**, Valtaoja, E., Tornikoski, M., Hovatta, T. and Kotiranta, M.

Although blazars have many common properties, they differ in one very basic respect: the preferred frequency of their emitted energy can vary from IR to X-ray domain. The goal of Paper I was to use as large a sample of BLOs as possible, determine their SEDs, and establish the range of the ν_p -values and see whether their distribution among BLOs was continuous. Such a straightforward study had not been done before. The samples used in similar analyses are usually considerably smaller. We used a sample of 398 BLOs, and for 308 we obtained a ν_p from a parabolic fit to the synchrotron component of the SED. The range of $\log \nu_p$ -values was from 12.67 to 21.46. There were 22 sources with $\log \nu_p > 19$. Although some of them may be genuine extreme HBLs, it is likely that the parabolic fit slightly exaggerates the peak frequency for HBLs.

The major result of Paper I was the lack of correlation between the peak frequencies and peak luminosities. This speaks strongly against the blazar sequence scenario, which depends upon the anticorrelation of the aforementioned quantities. The use of such a large sample of BLOs also proves the continuous nature of the population which before has been thought to consist of two inherently different groups, RBLs and XBLs.

We continued our work on SEDs in Paper IV. An often overlooked aspect when discussing possible correlations of the blazar population is the effect of Doppler boosting. It is usually assigned some fixed value or ignored completely. We set out to study its effect using a new set of Doppler factors derived from variability data (Hovatta et al. 2009). We used a sample of 135 radio-bright AGN, 65 of which are definite blazars. For consistency, we determined the SEDs for the whole sample anew although many of them had been included in the sample of Paper I. The resulting correlation between the Doppler boosting factors and the Doppler-corrected peak frequencies is striking. All extremely boosted sources have $\log \nu_p < 13.5$. When the dependency between ν_p and peak luminosities is determined with de-boosted quantities, the alleged anti-correlation turns in fact positive, completely contrary to the blazar sequence scenario. The stronger boosting of low ν_p -sources also explains the U-shaped distribution of the sample of Paper I in the $\nu_p - \nu_p L_p$ -plane. When the low ν_p -sources of Paper I are de-boosted, we find a very strong positive correlation among the BLO sample. This is remarkable, and deserves further investigation in future work. Although the positive correlation was unexpected, the implied stronger intrinsic luminosity of HBLs explains the puzzle of BLO number counts (Padovani 2007). According to the original blazar sequence, HBLs would be less luminous than LBLs, and thus, more numerous. Observational evidence, however, indicated that HBLs were a minority. This fits perfectly to our results.

7.2 Blazar long-term variability

Paper II: *37 GHz Observations of a Large Sample of BL Lacertae Objects*
by **Nieppola, E.**, Tornikoski, M., Lähteenmäki, A., Valtaoja, E., Hakala, T., Hovatta, T., Kotiranta, M., Nummila, S., Ojala, T., Parviainen, M., Ranta, M., Saloranta, P.-M., Torniainen, I. and Tröller, M.
Paper III: *Long-term radio variability of AGN: flare characteristics*
by Hovatta, T., **Nieppola, E.**, Tornikoski, M., Valtaoja, E., Aller, M. F. and Aller, H. D.
Paper V: *Long-term variability of radio-bright BL Lacertae objects*
by **Nieppola, E.**, Hovatta, T., Tornikoski, M., Valtaoja, E., Aller, M. F., Aller, H. D.

Using variability studies in the radio frequencies we can study the transient phenomena in the blazar synchrotron radiation. In Paper II we used a large sample of 398 BLOs to find out the typical flux levels of BLO emission at 37 GHz. The large sample size and the length of our observing period were an asset. Usually, observing periods are much shorter, or, even if monitoring lasts for several years, it is targeted at well-known and bright sources. Our results show that BLOs are typically very faint at 37 GHz. 34 % of the sources in the sample, mostly selected from Véron-Cetty & Véron (2000), were detected at $S/N > 4$. More than half of the detected sources were LBLs, while only 15% of HBLs were detected. The Metsähovi detection limit is of the order of 0.2 Jy in optimal weather conditions. A large majority of the sources had an average flux density below 1 Jy. We also reported the average variability indices for the sample and subgroups separately. They were surprisingly similar for both LBLs and HBLs, $\tilde{V}_{varI} = 0.32$ and $\tilde{V}_{varI} = 0.30$, respectively. Even if the fractional variability of the sources may be quite high, their absolute variability is typically very low. For a large majority, the amplitude of variability is 1 Jy at the most, and only for three sources, S5 0716+714, OJ 287 and BL Lac, it is of the order of several Jy.

The BLO observing campaign was initiated in order to facilitate the data reduction of the Planck satellite. With observational evidence of expected BLO fluxes, their emission can more easily be taken into account in the CMB data processing. The detection limit of Planck is very similar to that of Metsähovi (0.2 - 0.6 Jy), so the detection rates are directly comparable. One interesting result of our campaign was that even the faintest of BLOs seem to exhibit flaring. In some cases, there were several non-detections of the source, and then one clear detection, indicating a definite rise in the flux density. Also, the 5 to 37 GHz spectra of many faint sources having only one detection at 37 GHz were surprisingly inverted. This suggests that the measurement was taken in a high state. If the spectrum normally resembles the average, flat BLO spectrum, the quiescent flux density should be 50 mJy or less.

In Paper III and Paper V we approach the variability issue from a slightly different perspective. We have chosen a smaller sample of radio-bright objects and studied their flaring behaviour on a time scale of decades using 7 radio frequencies. The data were mostly obtained from the University of Michigan Radio Astronomy Observatory (UMRAO; 4.8, 8 and 14.5 GHz), Metsähovi Radio Observatory (22 and 37 GHz) and Swedish-ESO submillimetre Telescope (SEST; 90 and 230 GHz). The sample of Paper III consists of 55

AGN, most of which are blazars. 14 sources are BLOs, 20 HPQs, 12 LPQ and 4 galaxies. 5 additional sources were considered as LPQ due to lack of polarization measurements. In Paper V the whole sample comprises 24 BLOs, 13 of which had significant flaring during the observing period. Both papers concentrate on deriving central flare parameters, i.e. relative and absolute peak fluxes and duration, directly from the flux curves, and studying the typical range of flare behaviour in the sample. We also analyze the frequency evolution of the flares to conclude whether or not they adhere to the generalized shock model.

Paper III finds no definite differences in the flaring behaviour of the AGN subgroups, although there is weak evidence for longer lasting flares among LPQs. Both papers reach the conclusion that an average flare lasts for 2.5 years. Also, the Doppler-corrected peak flux of the flare does not depend on the duration of the flare, which indicates that the energy release does not increase in longer flares. The outbursts in both samples follow the generalized shock model, although analyzing the frequency evolution is made difficult by the ambiguous structure of the flares and the superposition of shock components. Paper V concludes that BLO flares are mostly high-peaking at 37 GHz and are likely to reach their maximum development in mm to sub-mm wavelengths. We also compared the correspondence between computational time scales (structure function, discrete correlation function and periodogram) and the observational flare parameters extracted directly from the flux curves (Paper V). There is a significant correlation between the two, but scatter is large. The deviation from one-to-one correspondence is easily 1 – 3 years.

References

Abdo, A. A., Ackermann, M., Ajello, M., et al. 2009, The Astrophysical Journal, 700, 597

Allen, S. W., Dunn, R. J. H., Fabian, A. C., Taylor, G. B., & Reynolds, C. S. 2006, Monthly Notices of the Royal Astronomical Society, 372, 21

Aller, M. F., Aller, H. D., & Hughes, P. A. 2003, The Astrophysical Journal, 586, 33

Aller, M. F., Aller, H. D., Hughes, P. A., & Latimer, G. E. 1999, The Astrophysical Journal, 512, 601

Antón, S. & Browne, I. W. A. 2005, Monthly Notices of the Royal Astronomical Society, 356, 225

Bade, N., Fink, H. H., & Engels, D. 1994, Astronomy & Astrophysics, 286, 381

Beckmann, V. 2003, in Astronomical Society of the Pacific Conference Series, Vol. 299, High Energy Blazar Astronomy, ed. L. O. Takalo & E. Valtaoja, 47–+

Blandford, R. D. & Königl, A. 1979, The Astrophysical Journal, 232, 34

Blandford, R. D. & Payne, D. G. 1982, Monthly Notices of the Royal Astronomical Society, 199, 883

Blandford, R. D. & Znajek, R. L. 1977, Monthly Notices of the Royal Astronomical Society, 179, 433

Błażejowski, M., Sikora, M., Moderski, R., & Madejski, G. M. 2000, The Astrophysical Journal, 545, 107

Bloom, S. D. & Marscher, A. P. 1996, The Astrophysical Journal, 461, 657

Bondi, M., Marchã, M. J. M., Dallacasa, D., & Stanghellini, C. 2001, Monthly Notices of the Royal Astronomical Society, 325, 1109

Brinkmann, W., Siebert, J., Kollgaard, R. I., & Thomas, H.-C. 1996, Astronomy & Astrophysics, 313, 356

Caccianiga, A. & Marchã, M. J. M. 2004, Monthly Notices of the Royal Astronomical Society, 348, 937

Ciaramella, A., Bongardo, C., Aller, H. D., et al. 2004, Astronomy & Astrophysics, 419, 485

Collinge, M. J., Strauss, M. A., Hall, P. B., et al. 2005, The Astronomical Journal, 129, 2542

Conway, J. E. & Wrobel, J. M. 1995, The Astrophysical Journal, 439, 98

D'Arcangelo, F. D., Marscher, A. P., Jorstad, S. G., et al. 2007, The Astrophysical Journal Letters, 659, L107

de Vries, W. H., Becker, R. H., & White, R. L. 2006, The Astronomical Journal, 131, 666

Dermer, C. D., Finke, J. D., Krug, H., & Böttcher, M. 2009, The Astrophysical Journal, 692, 32

Dermer, C. D. & Schlickeiser, R. 1993, The Astrophysical Journal, 416, 458

Donato, D., Ghisellini, G., Tagliaferri, G., & Fossati, G. 2001, Astronomy & Astrophysics, 375, 739

Dunlop, J. S., McLure, R. J., Kukula, M. J., et al. 2003, Monthly Notices of the Royal Astronomical Society, 340, 1095

Edelson, R., Turner, T. J., Pounds, K., et al. 2002, The Astrophysical Journal, 568, 610

Edelson, R. A. & Krolik, J. H. 1988, The Astrophysical Journal, 333, 646

Efstathiou, A. & Rowan-Robinson, M. 1995, Monthly Notices of the Royal Astronomical Society, 273, 649

Fanaroff, B. L. & Riley, J. M. 1974, Monthly Notices of the Royal Astronomical Society, 167, 31P

Ford, H. C., Harms, R. J., Tsvetanov, Z. I., et al. 1994, The Astrophysical Journal Letters, 435, L27

Fossati, G., Celotti, A., Ghisellini, G., & Maraschi, L. 1997, Monthly Notices of the Royal Astronomical Society, 289, 136

Fossati, G., Maraschi, L., Celotti, A., Comastri, A., & Ghisellini, G. 1998, Monthly Notices of the Royal Astronomical Society, 299, 433

Fritz, J., Franceschini, A., & Hatziminaoglou, E. 2006, Monthly Notices of the Royal Astronomical Society, 366, 767

Ghisellini, G. 1999, Astrophysical Letters Communications, 39, 17

Ghisellini, G., Celotti, A., Fossati, G., Maraschi, L., & Comastri, A. 1998, Monthly Notices of the Royal Astronomical Society, 301, 451

Ghisellini, G., Maraschi, L., & Tavecchio, F. 2009, Monthly Notices of the Royal Astronomical Society, 396, L105

Ghisellini, G. & Tavecchio, F. 2008, Monthly Notices of the Royal Astronomical Society, 387, 1669

Ghisellini, G., Tavecchio, F., & Chiaberge, M. 2005, Astronomy & Astrophysics, 432, 401

Ghisellini, G., Tavecchio, F., Foschini, L., et al. 2010, Monthly Notices of the Royal Astronomical Society, 402, 497

Gillessen, S., Eisenhauer, F., Trippe, S., et al. 2009, The Astrophysical Journal, 692, 1075

Gioia, I., Maccacaro, T., Schild, R., et al. 1990, The Astrophysical Journal Supplement Series, 72, 567

Giommi, P., Ansari, S. G., & Micol, A. 1995, Astronomy & Astrophysics Supplements, 109, 267

Giommi, P. & Padovani, P. 1994, Monthly Notices of the Royal Astronomical Society, 268, L51+

Giommi, P., Piranomonte, S., Perri, M., & Padovani, P. 2005, Astronomy & Astrophysics, 434, 385

Giommi, P., Tagliaferri, G., Beuermann, K., et al. 1991, The Astrophysical Journal, 378, 77

Giovannini, G., Cotton, W. D., Feretti, L., Lara, L., & Venturi, T. 2001, The Astrophysical Journal, 552, 508

Giroletti, M., Giovannini, G., Feretti, L., et al. 2004, The Astrophysical Journal, 600, 127

Hopkins, P. F., Richards, G. T., & Hernquist, L. 2007, The Astrophysical Journal, 654, 731

Hovatta, T., Nieppola, E., Tornikoski, M., et al. 2008, Astronomy & Astrophysics, 485, 51

Hovatta, T., Tornikoski, M., Lainela, M., et al. 2007, Astronomy & Astrophysics, 469, 899

Hovatta, T., Valtaoja, E., Tornikoski, M., & Lähteenmäki, A. 2009, Astronomy & Astrophysics, 494, 527

Hufnagel, B. R. & Bregman, J. N. 1992, The Astrophysical Journal, 386, 473

Hughes, P. A., Aller, H. D., & Aller, M. F. 1992, The Astrophysical Journal, 396, 469

Jannuzi, B. T., Smith, P. S., & Elston, R. 1994, The Astrophysical Journal, 428, 130

Kellermann, K. I. & Pauliny-Toth, I. I. K. 1969, The Astrophysical Journal Letters, 155, L71+

Kelly, B. C., Hughes, P. A., Aller, H. D., & Aller, M. F. 2003, The Astrophysical Journal, 591, 695

Kembhavi, A. K. & Narlikar, J. V. 1999, Quasars and active galactic nuclei : an introduction (Quasars and active galactic nuclei : an introduction /Ajit K. Kembhavi, Jayant V. Narlikar. Cambridge, U.K. : Cambridge University Press, c1999. ISBN 0521474779.)

Kharb, P. & Shastri, P. 2004, Astronomy & Astrophysics, 425, 825

Kidger, M. R. 2000, The Astronomical Journal, 119, 2053

Königl, A. 2007, in Revista Mexicana de Astronomia y Astrofisica Conference Series, Vol. 27, Revista Mexicana de Astronomia y Astrofisica, vol. 27, 91–101

Krolik, J. H. 2008, Memorie della Societa Astronomica Italiana, 79, 1003

Kühr, H. & Schmidt, G. 1990, The Astronomical Journal, 99, 1

Kühr, H., Witzel, A., Pauliny-Toth, I. I. K., & Nauber, U. 1981, Astronomy & Astrophysics Supplements, 45, 367

Lainela, M. & Valtaoja, E. 1993, The Astrophysical Journal, 416, 485

Laing, R. A., Bridle, A. H., Parma, P., et al. 2008, Monthly Notices of the Royal Astronomical Society, 386, 657

Landt, H. & Bignall, H. E. 2008, Monthly Notices of the Royal Astronomical Society, 391, 967

Landt, H., Padovani, P., & Giommi, P. 2002, Monthly Notices of the Royal Astronomical Society, 336, 945

Laurent-Muehleisen, S. A., Kollgaard, R. I., Feigelson, E. D., Brinkmann, W., & Siebert, J. 1999, The Astrophysical Journal, 525, 127

Ledden, J. E. & Odell, S. L. 1985, The Astrophysical Journal, 298, 630

Lehto, H. & Valtonen, M. J. 1996, The Astrophysical Journal, 460, 207

Lindfors, E. J., Türler, M., Valtaoja, E., et al. 2006, Astronomy & Astrophysics, 456, 895

Lomb, N. R. 1976, Astrophysics and Space Science, 39, 447

Londish, D., Croom, S. M., Boyle, B. J., et al. 2002, Monthly Notices of the Royal Astronomical Society, 334, 941

Londish, D., Croom, S. M., Heidt, J., et al. 2007, Monthly Notices of the Royal Astronomical Society, 374, 556

Maccacaro, T., Wolter, A., McLean, B., et al. 1994, Astrophysical Letters Communications, 29, 267

Malkan, M. A. & Sargent, W. L. W. 1982, The Astrophysical Journal, 254, 22

Marcha, M. J. M., Browne, I. W. A., Impey, C. D., & Smith, P. S. 1996, Monthly Notices of the Royal Astronomical Society, 281, 425

Marscher, A. P. 2009, ArXiv e-prints, 0909.2576

Marscher, A. P. & Gear, W. K. 1985, The Astrophysical Journal, 298, 114

Massaro, E., Giommi, P., Leto, C., et al. 2009, Astronomy & Astrophysics, 495, 691

Miyoshi, M., Moran, J., Herrnstein, J., et al. 1995, Nature, 373, 127

Morris, S. L., Stocke, J. T., Gioia, I. M., et al. 1991, The Astrophysical Journal, 380, 49

Nenkova, M., Sirocky, M. M., Nikutta, R., Ivezić, Ž., & Elitzur, M. 2008, The Astrophysical Journal, 685, 160

Nieppola, E., Hovatta, T., Tornikoski, M., et al. 2009, The Astronomical Journal, 137, 5022

Nieppola, E., Tornikoski, M., Lähteenmäki, A., et al. 2007, The Astronomical Journal, 133, 1947

Nieppola, E., Tornikoski, M., & Valtaoja, E. 2006, Astronomy & Astrophysics, 445, 441

Nieppola, E., Valtaoja, E., Tornikoski, M., Hovatta, T., & Kotiranta, M. 2008, Astronomy & Astrophysics, 488, 867

Ostorero, L., Villata, M., & Raiteri, C. M. 2004, Astronomy & Astrophysics, 419, 913

Padovani, P. 2007, Astrophysics and Space Science, 309, 63

Padovani, P., Costamante, L., Ghisellini, G., Giommi, P., & Perlman, E. 2002, The Astrophysical Journal, 581, 895

Padovani, P. & Giommi, P. 1995, The Astrophysical Journal, 444, 567

Padovani, P., Perlman, E. S., Landt, H., Giommi, P., & Perri, M. 2003, The Astrophysical Journal, 588, 128

Palma, C., Bauer, F. E., Cotton, W. D., et al. 2000, The Astronomical Journal, 119, 2068

Pauliny-Toth, I. I. K. & Kellermann, K. I. 1966, The Astrophysical Journal, 146, 634

Pauliny-Toth, I. I. K., Witzel, A., Preuss, E., et al. 1978, The Astronomical Journal, 83, 451

Perlman, E., Addison, B., Georganopoulos, M., Wingert, B., & Graff, P. 2008, PoS(BLAZARS2008)009

Perlman, E. S., Biretta, J. A., Sparks, W. B., Macchetto, F. D., & Leahy, J. P. 2001, The Astrophysical Journal, 551, 206

Perlman, E. S., Biretta, J. A., Zhou, F., Sparks, W. B., & Macchetto, F. D. 1999, The Astronomical Journal, 117, 2185

Perlman, E. S., Padovani, P., Giommi, P., et al. 1998, The Astronomical Journal, 115, 1253

Perlman, E. S. & Stocke, J. T. 1993, The Astrophysical Journal, 406, 430

Perlman, E. S., Stocke, J. T., Schachter, J. F., et al. 1996, The Astrophysical Journal Supplement Series, 104, 251

Pian, E., Urry, C. M., Maraschi, L., et al. 1999, The Astrophysical Journal, 521, 112

Plotkin, R. M., Anderson, S. F., Brandt, W. N., et al. 2009, ArXiv e-prints, 0911.0423

Plotkin, R. M., Anderson, S. F., Hall, P. B., et al. 2008, The Astronomical Journal, 135, 2453

Pyatunina, T. B., Kudryavtseva, N. A., Gabuzda, D. C., et al. 2006, Monthly Notices of the Royal Astronomical Society, 373, 1470

Pyatunina, T. B., Kudryavtseva, N. A., Gabuzda, D. C., et al. 2007, Monthly Notices of the Royal Astronomical Society, 381, 797

Raiteri, C. M., Villata, M., Aller, H. D., et al. 2001, Astronomy & Astrophysics, 377, 396

Raiteri, C. M., Villata, M., Kadler, M., et al. 2006, Astronomy & Astrophysics, 459, 731

Rawlings, S. & Saunders, R. 1991, Nature, 349, 138

Readhead, A. C. S. 1994, The Astrophysical Journal, 426, 51

Rees, M. J. 1966, Nature, 211, 468

Richards, G. T., Lacy, M., Storrie-Lombardi, L. J., et al. 2006, The Astrophysical Journal Supplement Series, 166, 470

Salonen, E., Teräsranta, H., Urpo, S., et al. 1987, Astronomy & Astrophysics Supplements, 70, 409

Sambruna, R. M., Gliozzi, M., Tavecchio, F., Maraschi, L., & Foschini, L. 2006, The Astrophysical Journal, 652, 146

Sambruna, R. M., Maraschi, L., & Urry, C. M. 1996, The Astrophysical Journal, 463, 444

Sbarufatti, B., Treves, A., & Falomo, R. 2005, The Astrophysical Journal, 635, 173

Scargle, J. D. 1982, The Astrophysical Journal, 263, 835

Schmitt, J. L. 1968, Nature, 218, 663

Shang, Z., Brotherton, M. S., Green, R. F., et al. 2005, The Astrophysical Journal, 619, 41

Sikora, M., Begelman, M. C., Madejski, G. M., & Lasota, J.-P. 2005, The Astrophysical Journal, 625, 72

Sikora, M., Begelman, M. C., & Rees, M. J. 1994, The Astrophysical Journal, 421, 153

Sillanpää, A., Haarala, S., Valtonen, M. J., Sundelius, B., & Byrd, G. G. 1988, The Astrophysical Journal, 325, 628

Simonetti, J. H., Cordes, J. M., & Heeschen, D. S. 1985, The Astrophysical Journal, 296, 46

Sokolov, A. & Marscher, A. P. 2005, The Astrophysical Journal, 629, 52

Soldi, S., Türler, M., Paltani, S., et al. 2008, Astronomy & Astrophysics, 486, 411

Sowards-Emmerd, D., Romani, R. W., Michelson, P. F., Healey, S. E., & Nolan, P. L. 2005, The Astrophysical Journal, 626, 95

Stevens, J. A., Litchfield, S. J., Robson, E. I., et al. 1994, The Astrophysical Journal, 437, 91

Stickel, M., Fried, J., & Kühr, H. 1993, Astronomy & Astrophysics Supplements, 98, 393

Stickel, M. & Kühr, H. 1996, Astronomy & Astrophysics Supplements, 115, 1

Stickel, M., Meisenheimer, K., & Kühr, H. 1994, Astronomy & Astrophysics Supplements, 105, 211

Stickel, M., Padovani, P., Urry, C. M., Fried, J. W., & Kühr, H. 1991, The Astrophysical Journal, 374, 431

Stocke, J. T., Morris, S. L., Gioia, I. M., et al. 1991, The Astrophysical Journal Supplement Series, 76, 813

Strittmatter, P. A., Serkowski, K., Carswell, R., et al. 1972, The Astrophysical Journal Letters, 175, L7+

Teräsranta, H., Achren, J., Hanski, M., et al. 2004, Astronomy & Astrophysics, 427, 769

Teräsranta, H., Tornikoski, M., Mujunen, A., et al. 1998, Astronomy & Astrophysics Supplements, 132, 305

Teräsranta, H., Tornikoski, M., Valtaoja, E., et al. 1992, Astronomy & Astrophysics Supplements, 94, 121

Teräsranta, H., Wiren, S., Koivisto, P., Saarinen, V., & Hovatta, T. 2005, Astronomy & Astrophysics, 440, 409

Tsang, O. & Kirk, J. G. 2007, Astronomy & Astrophysics, 463, 145

Türler, M., Courvoisier, T., & Paltani, S. 1999, Astronomy & Astrophysics, 349, 45

Türler, M., Courvoisier, T., & Paltani, S. 2000, Astronomy & Astrophysics, 361, 850

Turriziani, S., Cavazzuti, E., & Giommi, P. 2007, Astronomy & Astrophysics, 472, 699

Urry, C. M. & Padovani, P. 1995, Publications of the Astronomical Society of Pacific, 107, 803

Valtaoja, E., Teräsranta, H., Tornikoski, M., et al. 2000, The Astrophysical Journal, 531, 744

Valtaoja, E., Teräsranta, H., Urpo, S., et al. 1992, Astronomy & Astrophysics, 254, 71

Valtonen, M., Kidger, M., Lehto, H., & Poyner, G. 2008, Astronomy & Astrophysics, 477, 407

Valtonen, M. J., Nilsson, K., Villforth, C., et al. 2009, The Astrophysical Journal, 698, 781

van der Laan, H. 1966, Nature, 211, 1131

Véron-Cetty, M.-P. & Véron, P. 2000, A catalogue of quasars and active nuclei (A catalogue of quasars and active nuclei, 9th ed. Garching: European Southern Observatory (ESO), 2000, ESO Scientific Report no. 19.)

Veron-Cetty, M. P. & Veron, P. 2010, VizieR Online Data Catalog, 7258, 0

Villata, M. & Raiteri, C. M. 1999, Astronomy & Astrophysics, 347, 30

Vlahakis, N. & Königl, A. 2004, The Astrophysical Journal, 605, 656

Wolter, A., Caccianiga, A., della Ceca, R., & Maccacaro, T. 1994, The Astrophysical Journal, 433, 29

Wu, Z., Jiang, D. R., Gu, M., & Liu, Y. 2007, Astronomy & Astrophysics, 466, 63

Zirbel, E. L. & Baum, S. A. 1995, The Astrophysical Journal, 448, 521